Petrology, geochemical character and petrogenesis of a Variscan post-orogenic granite: case study from the Ševětín Massif, Moldanubian Batholith, Southern Bohemia

Petrologie, geochemický charakter a petrogeneze pozdně variské granitové intruze: příklady ze ševětínského masívu, moldanubický pluton, jižní Čechy

(16 figs, 6 tabs)

VOJTĚCH JANOUŠEK – STANISLAV VRÁNA – VOJTĚCH ERBAN

Czech Geological Survey, Klárov 3/131, 118 21 Prague 1, Czech Republic

In the composite Ševětín Massif (Moldanubian Zone of Southern Bohemia) three main granite pulses can be distinguished: (1) the oldest, two-mica Deštná granite with cordierite ± andalusite (SE part of the massif), (2) biotite–muscovite Ševětín granite (BMG), constituting most of the granite pluton, and (3) fine-grained biotite Ševětín granite (BtG) forming only minor bodies.

The Ševětín granites show transitional I/S type character. The whole-rock geochemical signature of the BtG is less evolved than that of the BMG. The former shows lower SiO_2, Na_2O, K_2O and A/CNK accompanied by higher TiO_2, FeO_t, MgO, Al_2O_3 and CaO. The BtG is also characterized by higher contents of Rb, Sr, Cr, Ni, La, LREE, Eu and Zr than the BMG.

The initial Sr isotopic ratios for four of the samples are nearly uniform regardless their petrology (BtG or BMG), showing fairly evolved character of the parental magmas ($^{87}Sr/^{86}Sr_{300}$ = 0.70922–0.70950) but sample BR 484 is even more radiogenic ($^{87}Sr/^{86}Sr_{300}$ = 0.71290). The initial epsilon Nd values are all highly negative (ε_{Nd}^{300} = –7.4 to –8.0; BR 484: ε_{Nd}^{300} = –9.2) and this is reflected by high two-stage Nd model ages (T_{Nd}^{DM} = 1.60–1.75 Ga).

Both the Ševětín granites (BtG and BMG) are coeval; their Sr–Nd isotopic compositions and whole-rock geochemistry correspond to a quartz–feldspathic (?metapsammitic) parentage or, more likely, may reflect a mixing between: (1) a relatively primitive component (having low time-integrated Rb/Sr and Sm/Nd ratios, with $^{87}Sr/^{86}Sr_i \leq 0.705$ and $\varepsilon_{Nd}^{i} = > -7$: e.g., undepleted or slightly enriched mantle derived melts or metabasic rocks) and (2) a material geochemically matching the mature Moldanubian metasedimentary rocks or their melts ($^{87}Sr/^{86}Sr_i > 0.713$ and $\varepsilon_{Nd}^{i} < -9.5$). Both BtG and BMG can be linked by up to *c.* 10 % of (nearly) closed system biotite–plagioclase fractional crystallization. The observed minor Nd isotopic heterogeneity could be explained by an influx of slightly isotopically and geochemically different melt batch(es) into periodically tapped and replenished magma chamber (RTF).

The Ševětín granites are probably fairly late, with indirect evidence suggesting their age comparable with Mauthausen Group in Austria (~300 Ma?). This is in line with occurrence of Ševětín granites next to late regional fault forming a part of the late Variscan Blanice Graben as well as comparable whole-rock geochemistry and Sr isotopic compositions of the Ševětín and Mauthausen granites (even though the Nd isotopic signatures of the two do differ profoundly). Moreover, the shallow intrusion level and rapid cooling are indicated also by the morphology of minute, long-prismatic zircon and apatite crystals and the Ab–Qz–Or normative plot.

Key words: granite, petrology, geochemistry, petrogenesis, Bohemian Massif, Variscides

Introduction

Strongly peraluminous post-orogenic granites (i.e. those with A/CNK = molar $Al_2O_3/(CaO + Na_2O + K_2O)$, higher than 1.1) form a conspicuous rock suite in the waning stages of the orogenic cycle. Various mechanisms of their origin were described (see Sylvester 1998 for a review). Two possible heat sources for the intracrustal melting are commonly accepted: the decay of radioactive elements in orogenic belts with substantial crustal thickening, and conduction/convection of mantle heat in 'thinner' belts. The former mechanism is capable of generating only small amounts of peraluminous granites (typical situation in HP–LT orogens e.g., Alps and Himalayas), whereas the latter is responsible for numerous strongly peraluminous intrusions in LP–HT orogenic belts, such as the Variscan (Sylvester 1998).

Within Central Europe, there are widespread volumetrically rather small post-orogenic calc-alkaline metaluminous and, more rarely, peraluminous granitoid plutons whose emplacement was connected with brittle tectonics (strike-slip and extensional faulting) developing at the final stage of the Variscan orogeny. Granitoids of this type (*c.* 310–290 Ma old group 4 of Finger *et al.* 1997) are relatively abundant in the Alpine–Carpathian realm, effectively rimming the southern flank of the orogen (Finger – Steyer 1990, Finger *et al.* 1997, Petrík – Kohút 1997, Uher – Broska 2000, Broska – Uher 2001). Within the Bohemian Massif they have been recognized in the Sudetes (e.g., the Liberec/Reichenberg granite: Kröner *et al.* 1994) and in the Moldanubian (or South Bohemian) Batholith (Mauthausen/Freistadt group: Frasl – Finger 1991, Finger *et al.* 1997, Gerdes 1997).

In the Czech part of the Moldanubian Batholith, petrographic and geochemical character similar to the Freistadt granodiorite from its classic occurrences in Austria has been ascribed to the Pavlov granite (15 km NW of Jihlava: Holub *et al.* 1995, Klečka – Matějka 1996, Matějka – Janoušek 1998) and Ševětín granites (20 km N of České Budějovice: Matějka 1991, Klečka – Matějka 1996, René *et al.* 1999). This paper aims – by means of combined study of petrology, whole-rock geochemistry and Sr–Nd isotopes – to contribute to discussion about classification and relative timing of the Ševětín granites, as well as to better understanding of the character and petrogenesis of late Variscan Moldanubian granitoids in general.

Regional setting

Moldanubian Batholith

The Moldanubian Batholith (MB; *c.* 6000 km^2) is the largest Variscan magmatic complex in the Bohemian Massif (Klečka – Matějka 1996). Granitoids of the MB intruded the Moldanubian Zone, a tectonic assemblage made of several crustal segments of contrasting age, ranging from Early Proterozoic to Early Palaeozoic. It consists of medium- to high-grade metamorphic rocks comprising mainly paragneisses and migmatites, with local intercalations of amphibolite, calc-silicate gneiss, quartzite, graphite schist and marble with granulite, serpentinite and other high-grade mafic bodies (Fiala *et al.* 1995 and references therein).

A review of plutonic rock types in the Moldanubian Batholith assumes the following relations (Frasl – Finger 1991, slightly modified by Klečka – Matějka 1996):

1 Group of older syn-orogenic granitoids (Early Carboniferous)
  1A Old S-types (Schärding, Peuerbach)
  1B Old I- and I/S (transitional) types (Weinsberg, Schlierengranit, quartz diorites and tonalites)
2 Group of younger syn-orogenic granitoids (Late Carboniferous)
  2A Locally slightly deformed S-types (Altenberg, Lásenice)
  2B Late I- and transitional I/S types (Freistadt, Mauthausen, Ševětín, Pavlov)
  2C Completely undeformed S types (Eisgarn group)
3 Subvolcanic felsic dykes
  3A Anorogenic granitoids (Homolka, Kozí Hora, Šejby)

Recently, a simplified genetic classification of the MB, taking into account the most recent petrologic, geochemical, isotopic and geochronological data, was published by Gerdes (1997):

A Rastenberg Plutons (RbP) (338–323 Ma)
  Metaluminous K-rich melagranites and melasyenites (Rastenberg, Třebíč, Jihlava)
B Weinsberg Granites (WbG) (328–318 Ma)
  Coarse-grained, porphyritic peraluminous granites (Weinsberg) with associated pyroxene-bearing cumulates (Sarleinsbach)
C Eisgarn Plutons (EsP) (327–318 Ma)
  Peraluminous two-mica granites (medium-grained porphyritic variety: EsG, even-grained variety: EsG-W, fine-grained varieties from Bohemia: EsG-M, EsG-N)
D Mauthausen Group (MG) (302–305 Ma)
  High-K calc-alkaline biotite granites to granodiorites (Freistadt: FGd, Plöcking: PlG, Mauthausen: MhG, Pfahl: PfG) with associated minor quartz diorite bodies

Ševětín Massif

The Ševětín Massif is a composite granitoid body that intruded as several pulses the Moldanubian Zone of Southern Bohemia. It is rather small but is expected to have a larger extent under the sedimentary cover (Šalan-

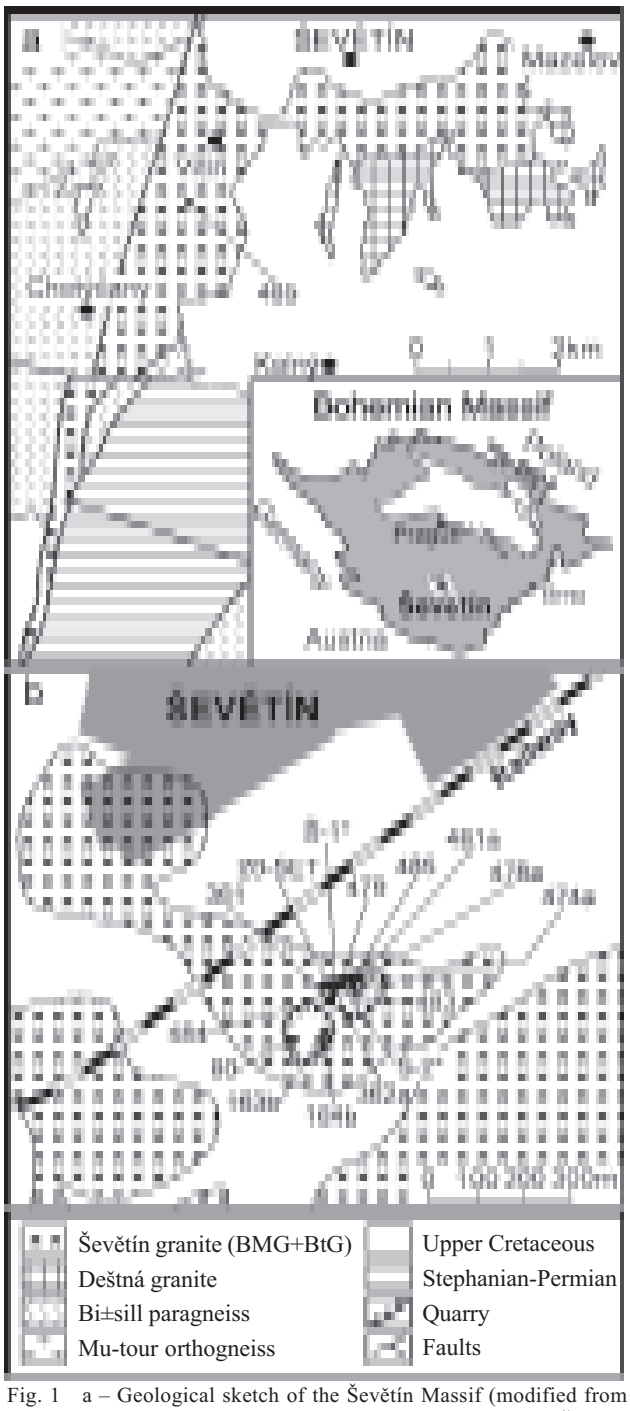

Fig. 1 a – Geological sketch of the Ševětín Massif (modified from the map 1 : 25 000, Suk *et al.* 1978); b – Detailed map of the Ševětín quarries and their immediate surroundings showing sample locations (samples Š-1*, Š-2* and 20-SET are from Matějka 1991; prefixes "BR" for samples collected in course of the present study were omitted for clarity).

ský in Suk *et al.* 1978). The Ševětín Massif is located along the eastern side of the Drahotěšice Fault Zone (Fig. 1), with the most extensive exposure near the village of Ševětín, 15 km NNE of České Budějovice. The body is L-shaped, with two perpendicular branches. The eastern one is about 5 km long, surrounded by Cretaceous sediments of the České Budějovice basin. The southern branch, *c.* 9 km long, is attenuated to a narrow (less than 1 km wide) spur between the Drahotěšice Fault Zone and Lhotice Graben (part of the Blanice Graben) of late Stephanian and Permian sediments (Suk *et al.* 1978, Matějka 1991) (Fig. 1).

Up till now, three granite pulses have been recognized and characterized near Ševětín:

(1) Two-mica granite, cordierite or cordierite–andalusite bearing (Deštná type – Klečka *et al.* 1991, René *et al.* 1999) forming the south-eastern part of the Ševětín Massif. The exposed part occupies *c.* 7 km^2, but it is largely covered by Upper Cretaceous sediments (Suk *et al.* 1978, Matějka 1991).
(2) Biotite–muscovite granite (BMG – Fig. 2), constituting the largest part of the granite pluton; the exposed part is *c.* 16 km^2 (Suk *et al.* 1978, Matějka 1991).
(3) Fine-grained biotite granite (BtG), confined to area approximately 100 by 200 m in the new Ševětín quarry.

This study deals with the latter two groups that have been considered to be two facies of a single Ševětín type (Ambrož 1935, Matějka 1991, René *et al.* 1999). Both the BMG and BtG will be termed in this text as Ševětín granites.

Chronology of the individual magma pulses in the Ševětín Massif

Two-mica Deštná granite has been correlated, on the geochemical and petrologic grounds, with the main occurrence of this granite type in the Klenov massif (René *et al.* 1999), 20 km NE of Ševětín. The two-mica granite belongs to the clan of Eisgarn type granites, whose age has been a matter of a considerable dispute.

An earlier whole-rock Rb–Sr dating of two-mica granites in the northern part of the Moldanubian Batholith by Scharbert – Veselá (1990) yielded a relatively young age of 303 ± 6 Ma. This age is unreliable, though, as their samples, covering a large region, involved several magma pulses each with a distinct source and petrogenesis (Matějka – Janoušek 1998, Scharbert 1998). In contrast, most workers now accept an older crystallization age for the great majority of the peraluminous two-mica granites in the MB. This is based on conventional U–Pb monazite age of 327 ± 4 Ma determined for Austrian Eisgarn granite by Friedl *et al.* (1996), as well as re-evaluation of earlier Rb–Sr WR data (Scharbert 1987) by Gerdes (1997: 324 ± 8 Ma), Rb–Sr whole-rock dating of Scharbert (1998: 330 ± 6.5 Ma), and Ar–Ar muscovite dating (328–320 Ma), recording cooling below *c.* 400–350 °C (Scharbert *et al.* 1997). This is in a good agreement with the dating of P-rich Homolka granite that is assumed to be a late fractionate of an Eisgarn-like melt (327 ± 4 Ma: Rb–Sr WR, 317 ± 2 and 315 ± 3 Ma: muscovite Ar–Ar; Breiter – Scharbert 1995).

Even though certainly younger than the Deštná intrusion, the ages of both Ševětín granites are not likely to differ remarkably. On the other hand, biotite–muscovite (BM) granite is intruded by a dyke of pyroxene microgranodiorite in the old Ševětín quarry (Vrána *et al.* 1993). The age of this dyke swarm, whose cooling has been dated at 274 Ma (amphibole Ar–Ar: Košler *et al.* 2001) constrains the minimum age for the BM granite.

In the absence of direct geochronological data, we infer from indirect evidence given by Matějka (1991) and below that the Ševětín granite probably belongs to the late Variscan group of granites similar in age to the biotite granodiorite of the Freistadt type dated at 302 ± 2 Ma (Friedl *et al.* 1992). On this basis the age 300 Ma has been used throughout this paper for calculation of initial isotopic ratios.

Field relations and petrography

Biotite–muscovite granite (BMG)

The medium- to fine-grained biotite–muscovite granite (BMG) has a speckled texture due to biotite clots up to 6 mm across, in part formed by replacement of cordierite

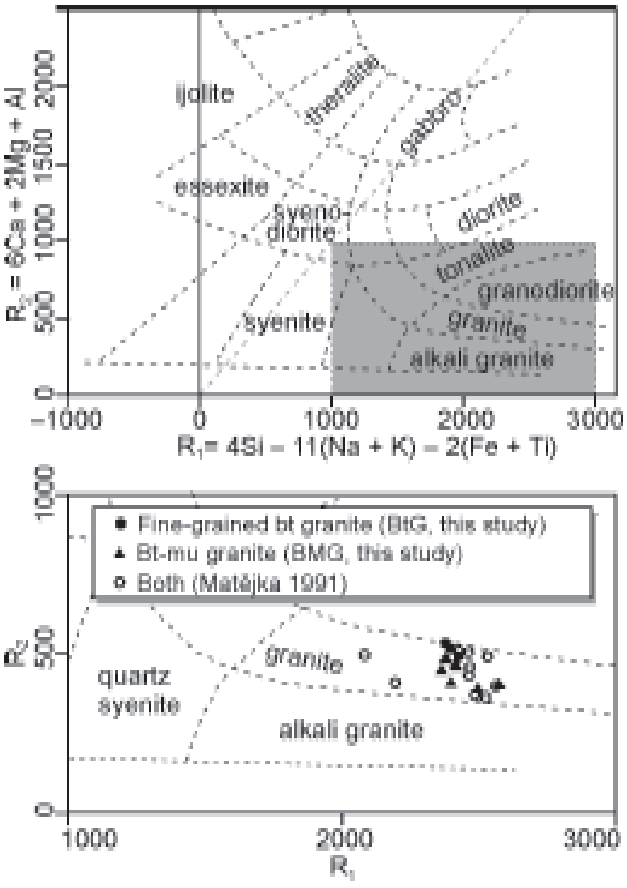

Fig. 2 Classification of the Ševětín granites in the multicationic diagram of De la Roche *et al.* (1980).

by biotite ± muscovite; in some samples, e.g. BR 80, fresh cordierite is preserved next to partly pinitized one. Other textural irregularities include minor aplitic or pegmatoid schlieren, and rare disseminated K-feldspar phenocrysts (or xenocrysts?) up to 1.5 cm across.

Rare enclaves include two rock types: (1) fine-grained biotite tonalite to granodiorite enclaves *c.* 10 cm across, characterized by increased normative albite, chloritized biotite and in some cases relatively abundant muscovite replacing plagioclase, and (2) biotite paragneiss xenoliths 15 cm to 5 metres across. The petrologic and geochemical character of the enclaves are beyond the scope of the current work – their chemical analyses are presented in Table 1.

Main constituents include subhedral plagioclase (0.5–3.5 mm), quartz (0.5–1.5 mm), anhedral and weakly perthitic K-feldspar (2.0–5.0 mm). Biotite (0.2–1.0 mm) is strongly pleochroic (X: light brown, Y=Z: foxy red brown). The granite contains minor to accessory muscovite, which appears to be typically of a late magmatic (deuteric) origin, but a few muscovite crystals are up to 1.5 mm long. Textural evidence indicates muscovite crystallization by replacement of cordierite, biotite and plagioclase. Relatively coarse muscovite, presumably primary, characteristic of Eisgarn type granites (D'Amico *et al.* 1981), appears to be absent. Highly characteristic is the unusually small size of zircon and apatite crystals. Slender long-prismatic zircon crystals are typically 1–5 by 10–50 μm in size.

Biotite–muscovite granite is strongly modified by late brittle fracturing, brecciation, formation of mm- to cm-wide microcataclasite veins and local hydrothermal silicification. In localized domains, the granite shows a strong deformation of quartz including quasi-planar rhombohedral cleavages, extinction patterns similar to microcline polysynthetic twinning and quasi-planar features similar to planar deformation features (Cordier *et al.* 1994). Deformations of this type, accompanied by relatively modest hydrothermal growth of quartz, chlorite and albite in granite cataclasites, correlate with position of this granite next to the Drahotěšice Fault Zone, with a probable lateral displacement of several kilometres. In the new Ševětín quarry, up to 5 m wide zone of quartz–fine-grained muscovite rock (> 90 wt % SiO_2) developed from granite. Fifty to one hundred metres wide zone of hydrothermal quartz and silicified breccias along the Drahotěšice Fault Zone show textures pointing to multiepisodic brecciation and silicification.

Samples of Ševětín granite used in this study were selected so that they are nearly free of this late cataclastic deformation and silicification imprint and were as fresh as possible.

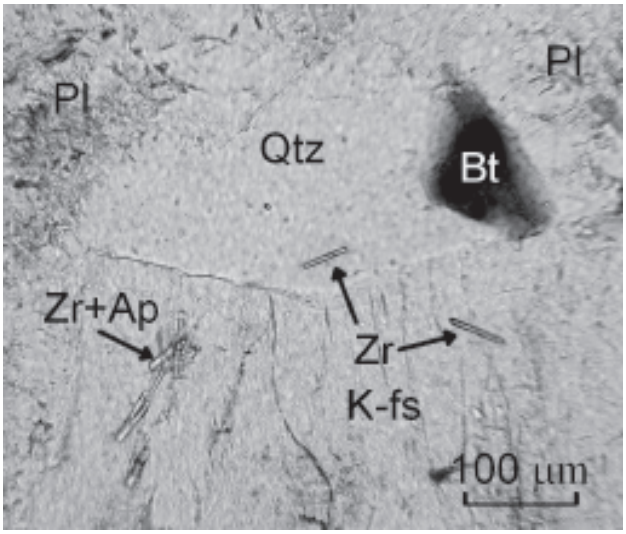

Fig. 3 Photomicrograph showing long prismatic/acicular morphology of zircon and apatite (Zr, Ap) in the biotite granite (BtG). K-fs: K-feldspar, Pl: plagioclase, Qtz: quartz, Bt: biotite. Sample 362A.

Fine-grained biotite granite (BtG)

The rock shows notably more regular subhedral morphology of plagioclase (0.2–1.0 mm), compared to biotite-muscovite granite. K-feldspar (0.3–1.2 mm) is anhedral and weakly perthitic. Biotite (0.1–0.4 mm), often chloritized, has dark pleochroic colours: Y = Z: brownish black, X: grey brown to light brown. Zircon and apatite show unusually small size, comparable to the BMG, and this indicates some similarities in evolution of both granite types. The abundance of minute long-prismatic to acicular zircon crystals is a striking microscopic feature (Fig. 3).

On the other hand, effects of intense dynamic cataclastic deformation including specific deformation phenomena in quartz, characteristic of the BMG, have not been observed in the fine-grained biotite granite. This relation suggests that the biotite granite was emplaced and solidified after a major deformation event affecting the biotite–muscovite granite. However, this relation is not considered as a safe proof of relative age of BMG and BG. On the contrary, Matějka (1991) has observed large xenoliths of the darker, finer grained biotite granite enclosed by the lighter biotite–muscovite granite.

Analytical techniques

Whole-rock chemical analyses were performed in the laboratories of the Czech Geological Survey (CGS), Prague, using procedures of wet analysis (J. Sixta, Chief chemist). Minor and trace element abundances were determined in the same laboratory by XRF (Cr, Ni, Cu, Zn, Rb, Sr, Y, Zr, Nb, Sn, Ba, Pb, U) and AAS (Be, Cr, Ni, Cu, Zn, Rb, Sr, Ba; samples 474a, 477a, 478a, and 481a). REE and Y were obtained by ICP OES Perkin-Elmer Plasma II (CGS).

For the isotopic study, samples were dissolved using a combined HF–HCl–HNO_3 attack. Strontium and bulk REE were isolated by standard cation-exchange chromatography techniques on quartz columns with BioRad res-

in, Nd was further separated on quartz columns with Biobeads S-X8 coated with HDEHP (Richard *et al.* 1976). Isotopic analyses were performed on Finnigan MAT 262 thermal ionization mass spectrometer in static mode using a double Re filament assembly (CGS). The $^{143}Nd/^{144}Nd$ ratios were corrected for mass fractionation to $^{146}Nd/^{144}Nd = 0.7219$, $^{87}Sr/^{86}Sr$ ratios assuming $^{86}Sr/^{88}Sr = 0.1194$. External reproducibility is given by results of repeated analyses of the La Jolla ($^{143}Nd/^{144}Nd = 0.511858 \pm 26$ (2σ), n = 18) and NBS 987 ($^{87}Sr/^{86}Sr = 0.710250 \pm 24$ (2σ), n = 10) isotopic standards.

The Rb and Sr concentrations, and the Rb/Sr ratios, were determined using XRF apparatus in the CGS by an approach similar to Harvey – Atkin (1981 and references therein). The Sm and Nd concentrations were obtained by ICP OES Perkin-Elmer Plasma II (CGS).

The decay constants applied to age-correct the isotopic ratios are from Steiger – Jäger (1977 – Sr) and Lugmair – Marti (1978 – Nd). The ε_{Nd} values and single-stage CHUR Nd model ages were obtained using Bulk Earth parameters of Jacobsen – Wasserburg (1980), the two-stage Depleted Mantle Nd model ages (T_{DM}^{Nd}) were calculated after Liew – Hofmann (1988).

For plotting, statistical calculations, recalculations of the isotopic data as well as numerical modelling of the whole-rock geochemical data, a freeware statistical package R was used (Ihaka – Gentleman 1996, Janoušek 2000a, b, R Development Core Team 2001).

Whole-rock geochemistry

Sample locations and whole-rock geochemical analyses obtained in course of this study are given in Table 1, the localities are also shown in Fig. 1. Whenever comparison is being made with typical Moldanubian two-mica granites, the data from unpublished database of D. Matějka are used. For these, available are only some Harker diagrams and binary plots involving trace elements (Matějka – Janoušek 1998, Figs 2 and 3, respectively).

Major elements

Compared to typical two-mica granites from the Czech part of the Moldanubian Batholith (Matějka unpublished data), the Ševětín granites display lower SiO_2, K_2O, K_2O/Na_2O and A/CNK values, coupled with higher CaO and Na_2O contents. The Boršov granite shows the same CaO, in principle comparable but slightly higher SiO_2 and slightly lower Na_2O, together with much higher K_2O and K_2O/Na_2O. The Pavlov granite is significantly less siliceous, being characterized by lower alkalis at analogous K_2O/Na_2O, A/CNK and higher CaO.

Both types of the Ševětín granites display conspicuous mutual differences in concentrations of some major elements. This can be best seen using the box and whiskers plots that portray realistically the statistical distribution of the geochemical data. The box represents 50 % of the population; the horizontal line inside it is the median (Fig. 4). For an interested reader, more detailed statistical information is given in a textual form (Table 2). As follows from the box and whiskers plots, the major-element character of the BtG is somewhat less evolved than that of the BMG. The former shows lower SiO_2, Na_2O and K_2O together with higher TiO_2, FeO_t, MgO, Al_2O_3 and CaO than the latter.

Identical information can be recovered from a single graph, the so-called biplot (Gabriel 1971, Buccianti – Peccerillo 1999). This useful but by geologists up till now largely overlooked diagram aims to represent both the observations and variables of a data matrix on the same bivariate plot. Inner products between variables approximate covariances and distances between observations approximate Mahalanobis distance (R Development Core Team 2001).

For the studied data set, the principal components analysis has been performed and its outcome (first two components) is shown in the form of such a biplot (Fig. 5a). The arrows express the main differences between the major-element compositions of the both Ševětín granites on the one hand and the Deštná granite on the other. Analyses of the Deštná granite from the Ševětín Massif (Matějka 1991, René *et al.* 1999) are significantly richer in silica and alkalis as well as poorer in all mafic components.

Additionally, some conclusions can be drawn concerning the correlations between major-element oxides. In a biplot, a comparable length and direction of two arrows imply that both elements are positively correlated; the opposite one indicates a strong negative correlation (Buccianti – Peccerillo 1999). This can be corroborated by

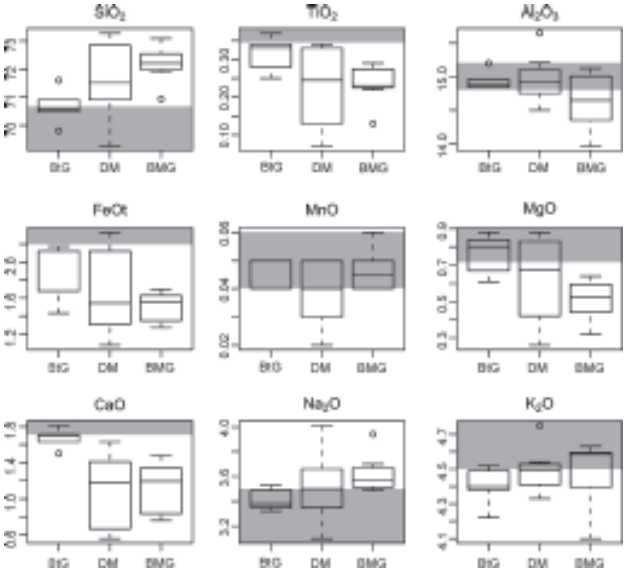

Fig. 4 Box and whiskers plots for wt % of major-element oxides in two main types of the Ševětín granites (BtG: biotite granite, 4 samples; BMG: biotite–muscovite granite: 8 samples; DM: Ševětín granites, not distinguished – Matějka 1991, 11 samples). See also Table 2. Shaded areas correspond to average composition of the Mauthausen granite (mean ± 1 standard deviation, 10 samples, see Table 2 of Vellmer – Wedepohl 1994).

Table 1 Whole-rock chemical composition of the granites of the Ševětín Massif

	Biotite-muscovite granite (BMG)									Fine-grained enclaves (mainly in BMG)				
	BR 163b	*BR 164b*	*BR 80*	*BR 474a*	*BR477a*	*BR 478a*	*BR 481a*	*BR 484*	*BR 485*	*BR 476b*	*BR 477b*	*BR 481b*	*BR 474b*	*BR 478b*
SiO_2	72.29	71.90	72.25	72.79	72.18	72.07	70.65	73.09	70.94	66.46	66.69	67.23	66.63	65.16
TiO_2	0.22	0.23	0.23	0.23	0.26	0.29	0.22	0.13	0.29	0.46	0.63	0.43	0.86	0.50
Al_2O_3	14.64	14.89	15.12	13.96	14.18	14.52	14.19	14.65	15.12	16.90	15.77	14.94	15.11	16.44
Fe_2O_3	0.13	0.05	0.17	0.52	0.73	0.70	0.63	0.28	0.43	0.81	0.99	1.51	1.27	0.93
FeO	1.39	1.55	1.25	0.83	0.99	0.98	0.87	1.02	1.31	2.22	3.28	3.29	3.13	3.23
MnO	0.048	0.054	0.046	0.042	0.040	0.043	0.092	0.059	0.038	0.061	0.082	0.253	0.084	0.069
MgO	0.48	0.54	0.40	0.51	0.64	0.62	0.49	0.32	0.57	1.31	1.68	1.86	2.02	1.98
CaO	1.29	1.10	1.48	0.76	0.83	1.30	1.64	0.84	1.38	1.22	0.81	1.14	1.54	3.30
Li_2O	0.018	0.020	0.055	0.006	0.011	0.014	0.008	0.018	0.012	0.020	0.034	0.028	0.027	0.038
Na_2O	3.59	3.64	3.70	3.49	3.94	3.55	4.28	3.53	3.50	4.54	5.09	5.32	3.08	3.69
K_2O	4.59	4.63	4.59	4.58	4.10	4.60	4.75	4.29	4.50	2.36	1.28	1.30	2.31	1.94
P_2O_5	0.21	0.20	0.19	0.14	0.14	0.15	0.15	0.22	0.127	0.22	0.19	0.17	0.62	0.20
CO_2	0.05	0.06	0.02	0.63	0.35	0.08	0.93	0.03	<0.01	0.53	0.29	0.50	0.80	0.09
C	0.01	0.01	0.01	0.02	0.05	0.01	0.03	0.02	0.03	0.12	0.07	0.03	0.06	0.03
F	0.060	0.030	0.070	0.040	0.050	0.060	0.060	0.040	0.064	0.090	0.060	0.060	0.090	0.160
S	0.03	0.04	0.01	0.01	0.02	0.02	0.02	0.01	0.01	0.02	0.03	0.03	0.02	0.03
H_2O^+	0.84	0.83	0.68	0.96	1.13	0.91	0.77	0.73	0.64	2.27	2.49	2.10	2.62	1.92
H_2O^-	0.05	0.09	0.18	0.15	0.16	0.21	0.11	0.15	0.19	0.22	0.26	0.19	0.16	0.19
Total	99.93	99.86	100.45	99.66	99.80	100.13	99.89	99.43	99.15	99.83	99.73	100.39	100.42	99.93
Be	–	–	–	4.8	7.8	7.2	9.3	9.5	6.4	9.0	8.3	13.7	7.2	7.1
Cr	–	–	–	21	12	21	11	14	8	23	50	78	94	34
Ni	–	–	–	11	10	7	<5	4	<2	7	9	14	62	8
Cu	–	–	–	3	5	5	6	5	5	4	4	4	9	7
Zn	–	–	–	75	82	43	75	35	45	67	89	187	157	104
Rb	–	–	–	178	168	191	213	204	226	182	89	76	165	176
Sr	–	–	–	211	228	262	144	132	323	–	–	–	–	–
Y	–	–	–	–	–	–	–	14.0	12.0	16.4	17.7	11.8	27.2	13.1
Zr	–	–	–	–	–	–	–	71	146	–	–	–	–	–
Nb	–	–	–	–	–	–	–	10	12	–	–	–	–	–
Sn	–	–	–	–	–	–	–	7	2	–	–	–	–	–
Ba	–	–	–	726	752	770	690	904	850	–	–	–	–	–
Pb	–	–	–	–	–	–	–	36	37	–	–	–	–	–
Cs	–	–	–	–	–	–	–	–	–	–	–	–	–	–
Th	–	–	–	–	–	–	–	–	–	–	–	–	–	–
U	–	–	–	–	–	–	–	3	3	–	–	–	–	–

	Biotite granite (BtG)						
	BR 361	*BR 362A*	*BR 479*	*BR 483*	*20-SET**	*Š-1**	*Š-2**
SiO_2	70.60	69.81	71.60	70.48	70.91	71.26	70.90
TiO_2	0.37	0.34	0.25	0.28	0.33	0.33	0.34
Al_2O_3	14.84	14.88	14.96	15.20	14.84	15.10	15.21
Fe_2O_3	0.08	0.08	1.18	0.44	0.60	0.42	0.45
FeO	2.05	2.10	0.37	1.28	1.58	1.95	1.89
MnO	0.049	0.048	0.040	0.053	0.044	0.046	0.040
MgO	0.84	0.88	0.67	0.61	0.80	0.83	0.86
CaO	1.70	1.81	1.50	1.71	1.63	1.41	1.50
Li_2O	0.015	0.018	0.010	0.015	–	–	–
Na_2O	3.35	3.32	3.49	3.53	3.38	3.18	3.10
K_2O	4.49	4.38	4.52	4.22	4.40	4.33	4.45
P_2O_5	0.12	0.13	0.14	0.14	0.16	0.12	0.12
CO_2	0.03	0.11	0.07	0.06	–	0.11	0.11
C	–	–	0.05	0.04	–	–	–
F	0.04	0.07	0.09	0.07	0.08	0.04	0.04
S	0.010	0.020	<0.005	0.040	–	–	–
H_2O^+	1.17	1.02	0.96	0.81	–	0.48	0.45
H_2O^-	0.10	0.11	0.11	0.14	–	–	–
Total	99.85	99.12	100.09	99.20	98.75	99.61	99.46
Be	–	–	–	–	–	–	–
Cr	–	–	–	17	42	–	–
Ni	–	–	–	3	–	–	–
Cu	<7	<7	–	5	–	–	–
Zn	41	40	–	45	41	47	61
Rb	214	200	–	200	201	190	210
Sr	254	280	–	303	266	273	274
Y	12.3	12.6	–	13	25	22	24
Zr	193	209	–	150	–	–	–
Nb	16	16	–	12	16	19	21
Sn	<7	<7	–	<2	–	–	–
Ba	1100	878	–	842	965	1249	1197
Pb	29	30	–	37	13	29	22
Cs	–	–	–	–	5	–	–
Th	–	–	–	–	22.9	–	–
U	–	–	–	6	6.8	–	–

* Analyses marked by an asterisk are from Matějka (1991)

Localities:

Biotite–muscovite granite (BMG)

BR 163b, BR 164b, BR 80 – Ševětín, old quarry (1983–1984)

BR 474a – Ševětín, new quarry, 50 m E of its NW corner (1995)

BR 477a, BR 478a, BR 481a – Ševětín, new quarry, 150 m E of its NW corner (1995)

BR 484 – Ševětín, new quarry, W margin (1996)

BR 485 – Vitín, quarry SSW of the village, W of the road (1996)

Fine-grained enclaves in the BMG

BR 476b – Ševětín, new quarry, 150 m E of its NW corner (1995), *c.* 7 cm across

BR 477b, BR 481b – Ševětín, new quarry, 150 m E of its NW corner (1995), enclaves *c.* 7 × 5 cm

BR 474b – Ševětín, new quarry, 50 m E of its NW corner (1995)

BR 478b – Ševětín, new quarry, 180 m E of its NW corner (1995), dark biotite gneiss xenolith 15 × 12 × 10 cm

Biotite granite (BtG)

BR 361 – Ševětín, new quarry, cut *c.* 12 m E of the quarry entry (1988)

BR 362A – Ševětín, new quarry, SW corner of an excavation *c.* 20–25 m SE of the quarry entry (1988)

BR 479 – Ševětín, new quarry, *c.* 150 m E of the SW corner (1995)

BR 483 – Ševětín, new quarry, pit at SE corner of the excavation (1996)

Table 2 Basic major-element statistics for granites of the Ševětín Massif (wt % except for A/CNK and A/NK that are in mol %)

Fine-grained biotite granite (BtG) (n=4)							
	Mean	*σ*	*Min*	*25%*	*50%*	*75%*	*Max*
SiO_2	70.62	0.74	69.81	70.31	70.54	70.85	71.60
TiO_2	0.31	0.05	0.25	0.27	0.31	0.35	0.37
Al_2O_3	14.97	0.16	14.84	14.87	14.92	15.02	15.20
FeOt	1.85	0.36	1.43	1.61	1.90	2.13	2.17
MnO	0.05	0.00	0.04	0.05	0.05	0.05	0.05
MgO	0.75	0.13	0.61	0.66	0.76	0.85	0.88
CaO	1.68	0.13	1.50	1.65	1.70	1.73	1.81
Na_2O	3.42	0.10	3.32	3.34	3.42	3.50	3.53
K_2O	4.40	0.14	4.22	4.34	4.44	4.50	4.52
K_2O/Na_2O	1.29	0.06	1.20	1.27	1.31	1.32	1.34
A/CNK	1.11	0.01	1.10	1.10	1.11	1.12	1.13
A/NK	1.44	0.03	1.41	1.42	1.44	1.46	1.47
Biotite–muscovite granite (BMG) (n=8)							
	Mean	*σ*	*Min*	*25%*	*50%*	*75%*	*Max*
SiO_2	72.19	0.64	70.94	72.03	72.22	72.42	73.09
TiO_2	0.24	0.05	0.13	0.23	0.23	0.27	0.29
Al_2O_3	14.63	0.42	13.96	14.43	14.64	14.95	15.12
FeOt	1.50	0.16	1.27	1.38	1.55	1.62	1.70
MnO	0.05	0.01	0.04	0.04	0.04	0.05	0.06
MgO	0.51	0.11	0.32	0.46	0.52	0.58	0.64
CaO	1.12	0.28	0.76	0.84	1.20	1.32	1.48
Na_2O	3.62	0.15	3.49	3.52	3.57	3.66	3.94
K_2O	4.49	0.19	4.10	4.45	4.58	4.59	4.63
K_2O/Na_2O	1.24	0.09	1.04	1.23	1.28	1.29	1.31
A/CNK	1.14	0.04	1.10	1.11	1.14	1.15	1.22
A/NK	1.35	0.04	1.30	1.33	1.35	1.38	1.42
Ševětín granite, undistinguished (Matějka 1991, René *et al.* 1999) (DM) (n=11)							
	Mean	*σ*	*Min*	*25%*	*50%*	*75%*	*Max*
SiO_2	71.55	1.28	69.26	70.91	71.26	72.76	73.28
TiO_2	0.24	0.10	0.07	0.17	0.26	0.33	0.34
Al_2O_3	14.95	0.31	14.50	14.79	14.84	15.07	15.65
FeOt	1.69	0.45	1.08	1.39	1.60	2.12	2.33
MnO	0.04	0.01	0.02	0.04	0.04	0.04	0.05
MgO	0.63	0.24	0.26	0.45	0.77	0.82	0.88
CaO	1.14	0.42	0.56	0.74	1.23	1.46	1.63
Na_2O	3.50	0.27	3.10	3.37	3.42	3.64	4.01
K_2O	4.48	0.11	4.33	4.41	4.49	4.52	4.75
K_2O/Na_2O	1.28	0.09	1.12	1.24	1.30	1.33	1.44
A/CNK	1.18	0.06	1.12	1.12	1.18	1.23	1.26
A/NK	1.41	0.07	1.29	1.37	1.41	1.44	1.53
Deštná granite from the Ševětín Massif (Matějka 1991, René *et al.* 1999) (n=5)							
	Mean	*σ*	*Min*	*25%*	*50%*	*75%*	*Max*
SiO_2	73.71	0.69	72.86	73.17	73.85	74.11	74.54
TiO_2	0.07	0.03	0.04	0.06	0.07	0.09	0.11
Al_2O_3	14.90	0.20	14.66	14.84	14.86	14.96	15.20
FeOt	0.63	0.27	0.36	0.42	0.54	0.88	0.94
MnO	0.02	0.01	0.01	0.01	0.02	0.02	0.02
MgO	0.21	0.05	0.15	0.15	0.23	0.25	0.25
CaO	0.42	0.11	0.29	0.33	0.47	0.51	0.52
Na_2O	3.55	0.25	3.11	3.60	3.64	3.71	3.71
K_2O	4.46	0.14	4.24	4.44	4.50	4.52	4.60
K_2O/Na_2O	1.26	0.10	1.18	1.21	1.24	1.24	1.43
A/CNK	1.31	0.08	1.24	1.25	1.27	1.33	1.44
A/NK	1.40	0.08	1.35	1.35	1.37	1.39	1.53

n = number of observations; σ = standard deviation; Min/Max = minimum/maximum;
50 %, 25 %, and 75 % = median and two quartiles

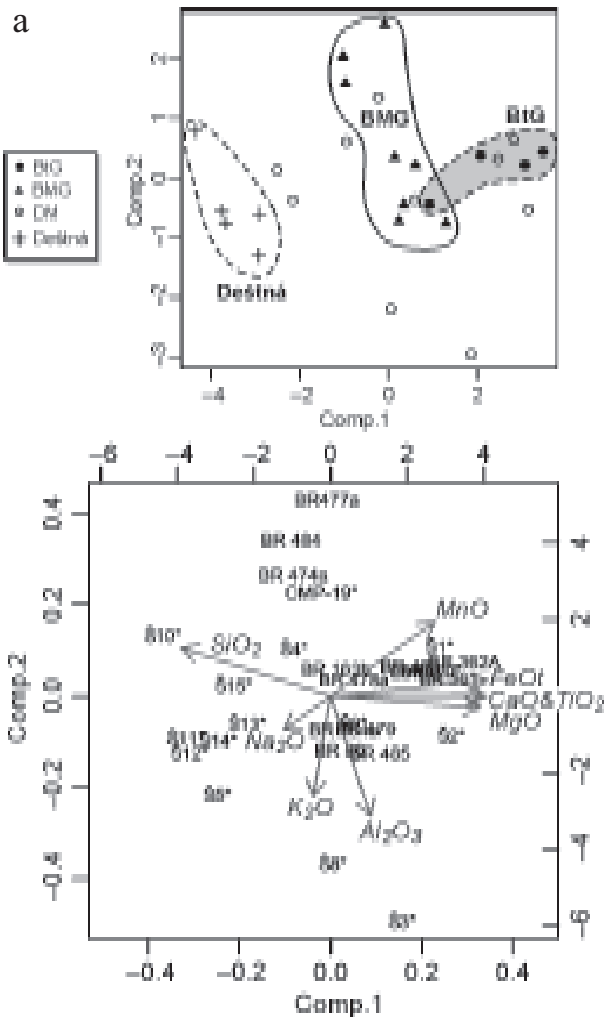

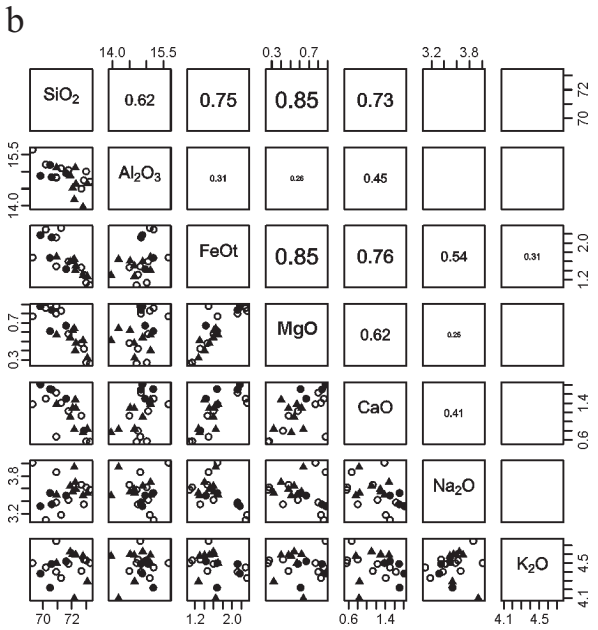

Fig. 5 a – Biplot of two principal components (Gabriel 1971, Buccianti – Peccerillo 1999) for granites from the Ševětín Massif (BtG: biotite granite; BMG: biotite–muscovite granite; DM: Ševětín granites, not distinguished – Matějka 1991, Deštná granite – Matějka 1991, René *et al.* 1999). The literature data are labelled by asterisks; b – Correlation plots for both types of the Ševětín granites (symbols as above); in addition, values of absolute correlations ≥ 0.25 are also shown (function `panel.core()`, see the entry for `pairs()` in the R manual: R Development Core Team 2001).

a more traditional set of binary plots, accompanied by absolute values of the correlation (Fig. 5b, only those ≥ 0.25 are presented). High positive correlation is shown by FeO_t/MgO and FeO_t/CaO pairs; negative by SiO_2/MgO, SiO_2/FeO_t and SiO_2/CaO.

In terms of the major-element whole-rock geochemistry, mode of occurrence and petrologic character, the Ševětín granites resemble Mauthausen granite from Austria (Fig. 4, shaded area corresponds to mean composition of the Mauthausen intrusion taken from Vellmer – Wedepohl 1994, their Table 2). Even though the Mauthausen granite is somewhat less siliceous, the similarity is striking.

The Ševětín granites are all slightly to moderately peraluminous, as their Shand's index (A/CNK) is significantly higher than 1.0 (Table 2). The BMG seem to be slightly more Al oversaturated than the BtG (BtG: A/NK = 1.10–1.13, mean = 1.11; BMG: A/CNK = 1.11–1.22, mean = 1.14) (Table 2).

Trace elements

Generally speaking, both the BtG and BMG are rich in Sr, Ba and LREE as well as poor in Rb relative to typical Czech two-mica granites (Matějka unpublished data).

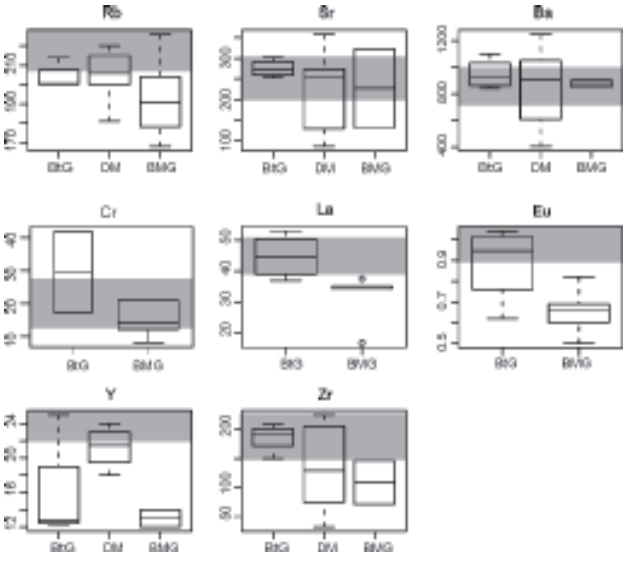

Fig. 6 Box and whiskers plots for trace-element concentrations (ppm) in the Ševětín granites (BtG: biotite granite, BMG: biotite–muscovite granite, DM: Ševětín granites, not distinguished – Matějka 1991, shown only, if enough data was available). See also Table 3. Shaded areas correspond to average composition of the Mauthausen granite (mean ± 1 standard deviation, 10 samples, see Table 2 of Vellmer – Wedepohl 1994).

Table 3 Basic trace-element statistics for granites of the Ševětín Massif (ppm)

Fine-grained biotite granite (BtG)									
	n	*NA*	*Mean*	*σ*	*Min*	*25%*	*50%*	*75%*	*Max*
Rb	3	1	204.7	8.1	200.0	200.0	200.0	207.0	214.0
Sr	3	1	279.0	24.5	254.0	267.0	280.0	291.5	303.0
Ba	3	1	940.0	139.7	842.0	860.0	878.0	989.0	1100.0
Cr	3	1	103.0	76.6	17.0	72.5	128.0	146.0	164.0
Ni	3	1	30.7	24.2	3.0	22.0	41.0	44.5	48.0
La	3	1	47.3	6.0	41.0	44.5	48.0	50.5	53.0
Eu	3	1	0.98	0.07	0.90	0.94	0.99	1.02	1.04
Y	3	1	12.63	0.35	12.30	12.50	12.60	12.80	13.00
Zr	3	1	184.0	30.5	150.0	171.5	193.0	201.0	209.0
Biotite–muscovite granite (BMG)									
	n	*NA*	*Mean*	*σ*	*Min*	*25%*	*50%*	*75%*	*Max*
Rb	5	3	193.4	22.7	168.0	178.0	191.0	204.0	226.0
Sr	2	6	227.50	135.10	132.00	179.75	227.50	275.25	323.00
Ba	2	6	877.0	38.2	850.0	863.5	877.0	890.5	904.0
Cr	5	3	15.2	5.7	8.0	12.0	14.0	21.0	21.0
Ni	4	4	8.00	3.20	4.00	6.25	8.50	10.25	11.00
La	5	3	31.8	8.5	16.8	34.4	35.0	35.1	37.6
Eu	5	3	0.65	0.12	0.50	0.60	0.66	0.69	0.82
Y	2	6	13.00	1.41	12.00	12.50	13.00	13.50	14.00
Zr	2	6	108.50	53.00	71.00	89.75	108.50	127.25	146.00
Ševětín granite, undistinguished (Matějka 1991, René *et al.* 1999) (DM)									
	n	*NA*	*Mean*	*σ*	*Min*	*25%*	*50%*	*75%*	*Max*
Rb	11	0	204.6	12.0	181.0	200.5	202.0	214.5	220.0
Sr	11	0	227.1	96.4	87.0	146.0	266.0	273.5	358.0
Ba	11	0	853.5	287.2	404.0	664.0	940.0	1008.5	1249.0
Cr	1	10	42.0	–	–	–	–	–	–
Y	9	2	21.7	2.4	18.0	20.0	22.0	24.0	25.0
Zr	10	1	132.5	69.2	32.0	83.25	129.5	190.25	225.0
Deštná granite from the Ševětín Massif (Matějka 1991, René *et al.* 1999)									
	n	*NA*	*Mean*	*σ*	*Min*	*25%*	*50%*	*75%*	*Max*
Rb	5	0	239.0	10.2	227.0	233.0	236.0	247.0	252.0
Sr	5	0	96.8	38.6	530.0	75.0	88.0	115.0	153.0
Ba	5	0	387.6	155.2	168.0	344.0	366.0	479.0	581.0
Y	5	0	25.8	6.5	22.0	22.0	22.0	26.0	37.0
Zr	5	0	44.4	13.8	33.0	34.0	36.0	59.0	60.0

n = number of observations; NA = not available; σ = standard deviation;
Min/Max = minimum/maximum; 50 %, 25 %, and 75 % = median and two quartiles

In these elements, the Ševětín granites bear a strong resemblance to the signature of the Boršov granite. The Ba concentrations are analogous, Rb is higher and Sr lower than in the Pavlov intrusion.

As shown by the box and whiskers plots (Fig. 6) and Table 3, the trace-element signature of the BtG is less evolved than that of the BMG. This can be demonstrated by the higher contents of Rb, Sr, Cr, Ni, La, Eu and Zr of the former. On the other hand, Ba concentrations do not differ greatly. Again, the similarity in trace-element composition between the Ševětín and Mauthausen granites is remarkable (Fig. 6).

As can be inferred from Table 4 and Fig. 7, the BtG shows significantly higher total REE contents and steeper REE patterns (Ce_N/Yb_N = 17.3–22.8, chondrite composition according to Boynton 1984) than the BMG (Ce_N/Yb_N = 6.7, but most samples contain Yb too low to be determined) (Figs 6 and 7). This is mainly due to significant differences in LREE and MREE concentrations between both groups (BtG higher than BMG), while the HREE remain virtually constant. Both types show pronounced negative Eu anomalies, with those for the BMG being slightly deeper (BtG: Eu/Eu* = 0.64–0.70, BMG: 0.56–0.62)

Sr–Nd isotope geochemistry

Newly obtained Sr–Nd isotopic data, age-corrected to 300 Ma, are summarized in Table 5. Even though the geochronological information is so far lacking, uncertainties in the age as high as 20 Ma make insignificant differences to the values calculated, especially for Nd isotopes (less than ± 0.3 ε unit).

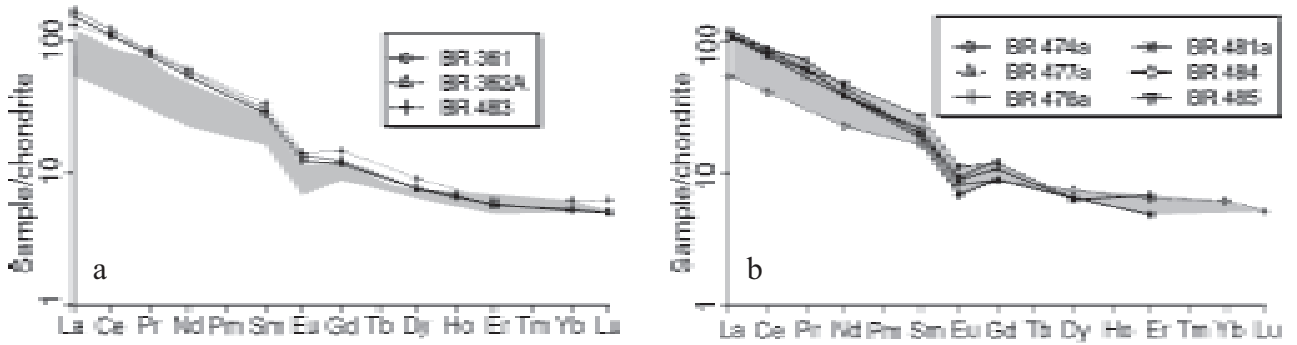

Fig. 7 Chondrite-normalized REE patterns for the Ševětín granites (a: biotite granite; b: biotite–muscovite granite); composition of the CI chondrite used for normalization is from Boynton (1984). Shaded field of the BM granite is shown on both plots for comparison.

With a notable exception of the sample BR 484 (BMG, $^{87}Sr/^{86}Sr_{300}$ = 0.71290), the initial Sr ratios are nearly uniform, showing fairly evolved character of the parental magmas ($^{87}Sr/^{86}Sr_{300}$ = 0.70922–0.70950). Similar pattern is followed also by the Nd isotopic compositions expressed as initial epsilon values that are all highly negative (ε_{Nd}^{300} = –7.4 to –8.2; for BR 484 is ε_{Nd}^{300} = –9.2). High two-stage depleted mantle model ages indicate a negligible (if any) role for depleted-mantle derived magmas and long crustal history of the protolith (two-stage T_{DM}^{Nd} = 1.60–1.65 Ga, for BR 484 is T_{DM}^{Nd} = 1.74 Ga).

The different (more evolved) isotopic composition of the sample BR 484 is difficult to explain. As the analysis seems to be a reliable one, it may indicate heterogeneity of the Ševětín granites beyond the scope of this – in terms of isotopic work inevitably highly limited – contribution. As will be shown later, the heterogeneity disclosed by this sample may be of a real petrogenetic importance.

The results from Ševětín, together with additional data for selected granitoid intrusions from the Moldanubian Batholith (Liew *et al.* 1989, Vellmer – Wedepohl 1994, Gerdes 1997, Matějka – Janoušek 1998) and for typical Moldanubian country rocks (mainly paragneisses and migmatites: Scharbert – Veselá 1990, Janoušek *et al.* 1995 and unpublished data), are plotted onto a $^{87}Sr/^{86}Sr_{300}$ versus

Table 4 Rare earth element concentrations in granites from the Ševětín Massif (ppm and normalized by chondrite – Boynton 1984)

	BtG			**BMG**				
	BR 361	*BR 362A*	*BR 483*	*BR 474a*	*BR477a*	*BR 478a*	***B**R 484*	*BR 485*
La	48.0	53.0	41.0	37.6	34.4	35.0	16.8	35.1
Ce	88.0	98.0	86.9	71.3	61.9	66.6	33.4	70.1
Pr	9.5	9.9	10.5	8.8	7.4	7.7	NA	7.5
Nd	32.0	35.0	36.3	26.8	23.6	23.5	13.6	28.6
Sm	5.5	5.9	6.5	3.8	4.2	3.9	3.2	5.3
Eu	0.90	0.99	1.04	0.69	0.66	0.60	0.50	0.82
Gd	3.0	3.2	3.8	3.2	2.8	2.3	2.3	3.1
Dy	2.43	2.45	2.90	NA	2.04	NA	2.40	2.10
Ho	0.47	0.49	NA	NA	NA	NA	NA	NA
Er	1.21	1.18	1.30	NA	1.44	1.02	1.35	NA
Yb	1.08	1.11	1.30	NA	NA	NA	1.30	NA
Lu	0.16	0.16	0.20	NA	NA	NA	0.17	NA
La_N	154.84	170.97	132.26	121.29	110.97	112.90	54.19	113.23
Ce_N	108.91	121.29	107.55	88.24	76.61	82.43	41.34	86.76
Pr_N	77.87	81.15	86.07	72.13	60.66	63.11	NA	61.48
Nd_N	53.33	58.33	60.50	44.67	39.33	39.17	22.67	47.67
Sm_N	28.21	30.26	33.33	19.49	21.54	20.00	16.41	27.18
Eu_N	12.24	13.47	14.15	9.39	8.98	8.16	6.80	11.16
Gd_N	11.74	12.36	14.67	12.36	10.81	8.88	8.88	11.97
Dy_N	7.55	7.61	9.01	NA	6.34	NA	7.45	6.52
Ho_N	6.55	6.82	NA	NA	NA	NA	NA	NA
Er_N	5.76	5.62	6.19	NA	6.86	4.86	6.43	NA
Yb_N	5.17	5.31	6.22	NA	NA	NA	6.22	NA
Lu_N	4.97	4.97	6.21	NA	NA	NA	5.28	NA
Eu/Eu*	0.67	0.70	0.64	0.61	0.59	0.61	0.56	0.62
Ce_N/Yb_N	21.08	22.84	17.29	NA	NA	NA	6.65	NA

BMG = Biotite–muscovite granite, BtG = Fine-grained biotite granite, NA = not available

Table 5 Sr-Nd isotopic data for granitoids from the Ševětín Massif

Sample	Rb (ppm)	Sr (ppm)	$^{87}Rb/^{86}Sr$	$^{87}Sr/^{86}Sr$	2 s.e.	$(^{87}Sr/^{86}Sr)_i$
Fine-grained biotite granite (BtG)						
BR 361	187	284	1.9085	0.717492	34	0.709344
BR 479	227	293	2.2468	0.719095	16	0.709503
BR 483	200	303	1.9123	0.717656	26	0.709492
Biotite-muscovite granite (BMG)						
BR 484	204	132	4.4837	0.732045	38	0.712904
BR 485	226	323	2.0271	0.717877	25	0.709223
Pyroxene microgranodiorite, Dehetník						
BR 486	118	322	1.0611	0.712004	16	0.707853

Sample	Sm (ppm)	Nd (ppm)	$^{147}Sm/^{144}Nd$	$^{143}Nd/^{144}Nd$	2 s.e.	$(^{143}Nd/^{144}Nd)_i$	ε^i_{Nd}	T^{Nd}_{CHUR} (Ga)	T^{Nd}_{DM} (Ga)
Fine-grained biotite granite (BtG)									
BR 361	4.2	25.5	0.09956	0.512026	40	0.511830	–8.2	0.96	1.67
BR 479	3.2	18.5	0.10456	0.512080	29	0.511875	–7.4	0.92	1.60
BR 483	6.5	36.3	0.10796	0.512053	8	0.511841	–8.0	1.01	1.65
Biotite–muscovite granite (BMG)									
BR 484	3.2	13.6	0.14155	0.512059	18	0.511781	–9.2	1.60	1.74
BR 485	5.3	28.6	0.11160	0.512063	8	0.511844	–8.0	1.03	1.65
Pyroxene microgranodiorite, Dehetník									
BR 486	5.3	27.9	0.11424	0.512239	20	0.512033	–4.9	0.74	1.39

Isotopic ratios with subscript 'i' were all age-corrected to 300 Ma with exception of the pyroxene microgranodiorite BR 486 for which the Ar–Ar age 275 Ma has been adopted (Košler *et al.* 2000); T^{Nd}_{DM} = two-stage Nd model ages calculated after Liew and Hofmann (1988).

ε^{300}_{Nd} diagram (Fig. 8). The Sr isotopic composition of the Ševětín granites is more radiogenic than most of the Mauthausen Group (Liew *et al.* 1989, Gerdes 1997), being comparable to its most acidic member, i.e. Mauthausen granite in Austria (see also Fig. 9). Remarkably similar composition is shown by the fine-grained biotite–muscovite Boršov granite from the Czech part of the Moldanubian Batholith (Matějka – Janoušek 1998). On the other hand, most of the Ševětín granites are more primitive in terms of their Sr isotopic composition than a majority of typical S-type two-mica granites of the Eisgarn family (notably Eisgarn s.s., Číměř, Čeřínek, Světlá, Lipnice – see Matějka – Janoušek 1998 for terminology). All Ševětín granites show highly negative ε values, much lower than granitoids of the Mauthausen Group (Figs 8–10) but, with the exception of BR 484, comparable to Boršov granites.

Geochemical modelling

In theory, linear trends observed in numerous binary plots of major-element whole-rock compositions of the Ševětín granites could have been caused by restite unmixing (e.g., Chappell *et al.* 1987). However, this scenario can be ruled out as the A/CNK values do not decrease with fractionation (e.g., MgO–A/CNK plot, Fig. 11) (Barbarin 1996).

On the other hand, sharp decrease in Sr and Ba with decreasing MgO (Fig. 11) indicates an important role for fractionation dominated by biotite and feldspars. Moreover, the sharp decrease of Zr with decreasing MgO indicates that the melt was saturated in respect to zircon and crystallized this mineral throughout its history, as does the decrease in LREE point to fractionation of monazite (Fig. 11, see also Ayres – Harris 1997, René *et al.* 1999).

The fractional crystallization hypothesis has been tested using the major-element modelling based on the general least-squares mixing equation of Bryan *et al.* (1969). It was performed by our own R language-based routines (Janoušek 2000a), using an approach analogous to Janoušek *et al.* (2000). Examples of the output are given in Table 6 and plotted in Fig. 12. The modelling has shown that most of the major-element compositional variation observed within the Ševětín granites can be modelled by up to 11 % fractional crystallization of biotite (56.6–62.3 %) and plagioclase (37.8–44.9 %) from a parental composition corresponding to sample Š-2 (Matějka 1991). The modelled fractionated melts included BR 484 (Table 1), as well as Š-4, Š-13 and Š-15 (Matějka 1991). The fit in all cases was reasonable to excellent (R^2 = 0.52–1.19).

Discussion

Classification, petrology and geochemical character of the Ševětín granites

Contrary to earlier thoughts and in agreement with Matějka (1991 and references therein) and René *et al.* (1999), the petrology, whole-rock major- and trace-element geochemistry coupled with Sr–Nd isotopic signature indicate completely distinct character, source and petrogenesis of the both Ševětín granites on the one hand and the Eisgarn suite on the other. However, the conclusion of Matějka (1991) and René *et al.* (1999) that the Ševětín type granitoids comprise granites–granodiorites, analogous to Freistadt granodiorites from their classic occurrences in Austria, does not seem to be fully justified.

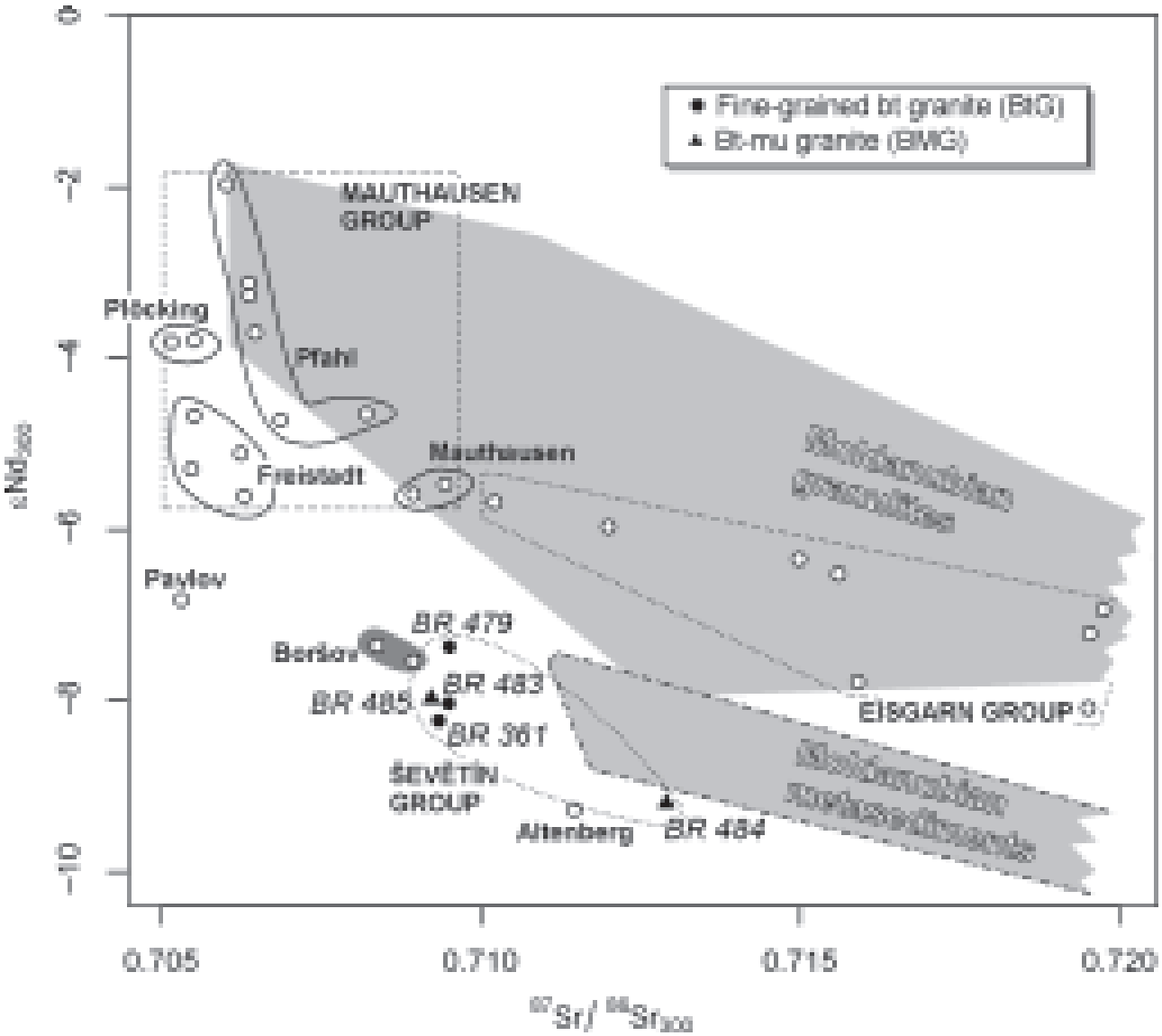

Fig. 8 $(^{87}Sr/^{86}Sr)_{300}$ versus ε_{Nd}^{300} plot for Ševětín granites. Plotted are also analyses of selected granitoids from the Moldanubian batholith (Liew *et al.* 1989, Vellmer – Wedepohl 1994, Gerdes 1997, Matějka – Janoušek 1998) and their country rocks (Scharbert – Veselá 1990, Valbracht *et al.* 1994, Janoušek *et al.* 1995 and unpublished data)

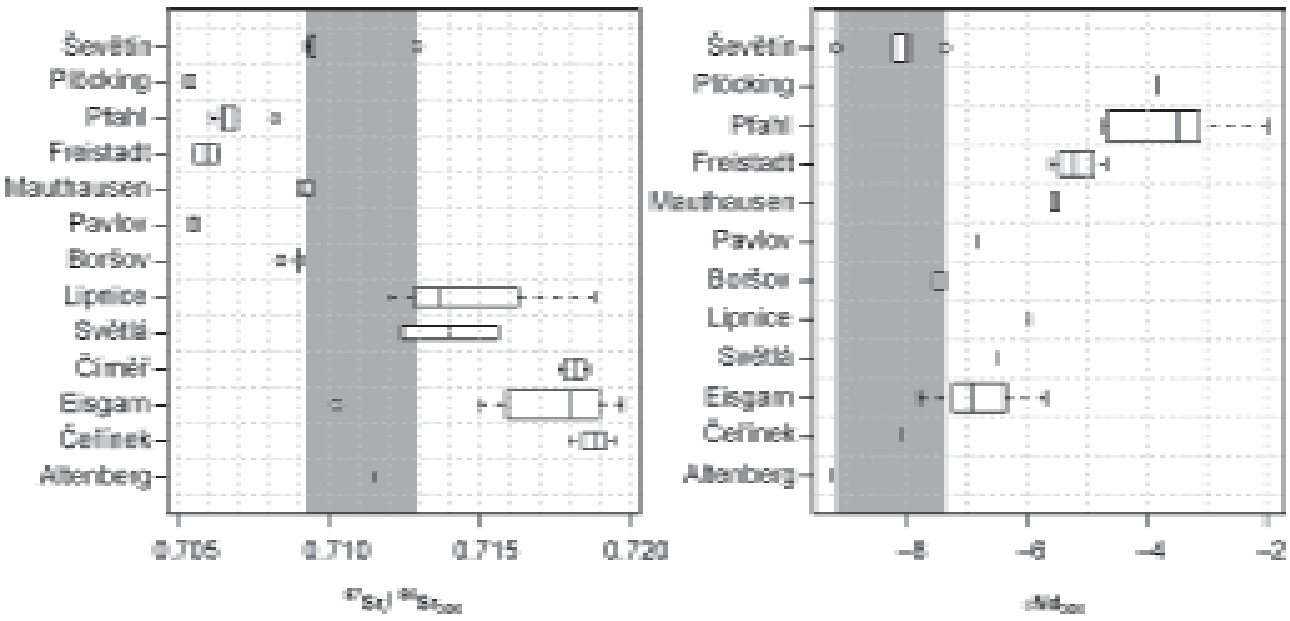

Fig. 9 Box and whiskers plots of initial $^{87}Sr/^{86}Sr$ ratios and ε_{Nd} values. See Fig. 8 for the data sources (all age-corrected to 300 Ma). Shaded region corresponds to the total range of the Ševětín granites (BtG and BMG, this study)

The idea that the Ševětín type includes granodiorites rests upon old, now abandoned classification scheme as well as several modal analyses, included in René *et al.* (1999), that are doubtful since they are at variance with the whole-rock chemistry. With no exception, all the analyses for the Ševětín granite presented by Matějka (1991; and thus also René *et al.* 1999) as well as those obtained in course of the present study correspond to granite (e.g., Fig. 2). While the Ševětín type granites are similar in appearance to Freistadt granodiorites and it is suggested on evidence given below that they are more or less closely similar in age, the petrochemical and Sr–Nd isotopic data presented in this article show substantial differences. However, Mauthausen granite, probably intimately petrogenetically related to the Freistadt intrusion (both forming members of the same suite termed by Gerdes 1997 the Mauthausen Group) resembles the Ševětín granites much more closely, save its less negative ε^{i}_{Nd} values that point probably to a different, less mature source.

As noted already by René *et al.* (1999) the A/CNK values for the Ševětín granites are much lower than

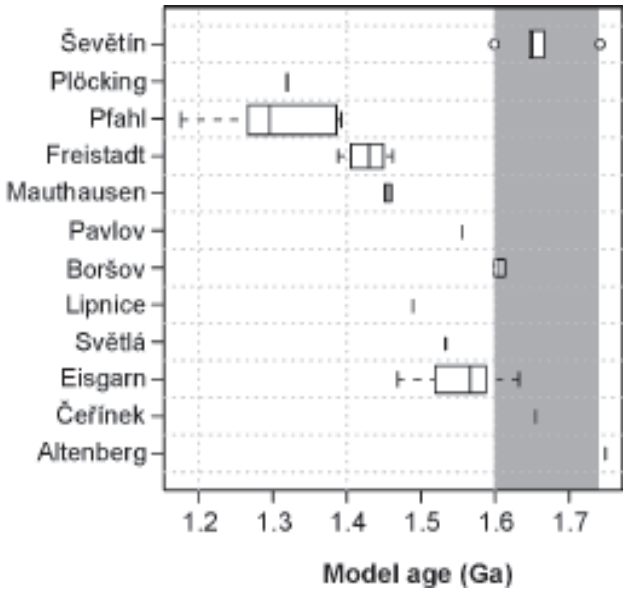

Fig. 10 Compilation of two-stage (Liew – Hofmann 1988) depleted-mantle Nd model ages for selected granitoid intrusions within the Moldanubian Batholith. See Fig. 8 for the data sources.

Table 6 Example of major-element based modelling of fractional crystallization using the least-squares approach of Bryan *et al.* (1969)

	Parent (Š-2)	Biotite	Plag.	Daughter (BR 484)	Calculated daughter	Diff.	Cumulate
SiO_2	70.19	36.74	61.60	73.09	72.98	0.11	47.52
TiO_2	0.34	4.69	0.00	0.13	0.05	0.08	2.66
Al_2O_3	15.21	19.45	24.48	14.65	14.42	0.23	21.63
FeOt	2.29	21.30	0.08	1.27	1.09	0.19	12.10
MgO	0.86	8.08	0.00	0.32	0.40	–0.08	4.58
CaO	1.50	0.00	6.83	0.84	1.32	–0.48	2.96
Na_2O	3.10	0.41	6.43	3.53	3.11	0.42	3.02
K_2O	4.45	8.65	0.58	4.29	4.36	–0.07	5.15
% in cumulate:			56.60	43.40			
$R^2 = 0.52$							

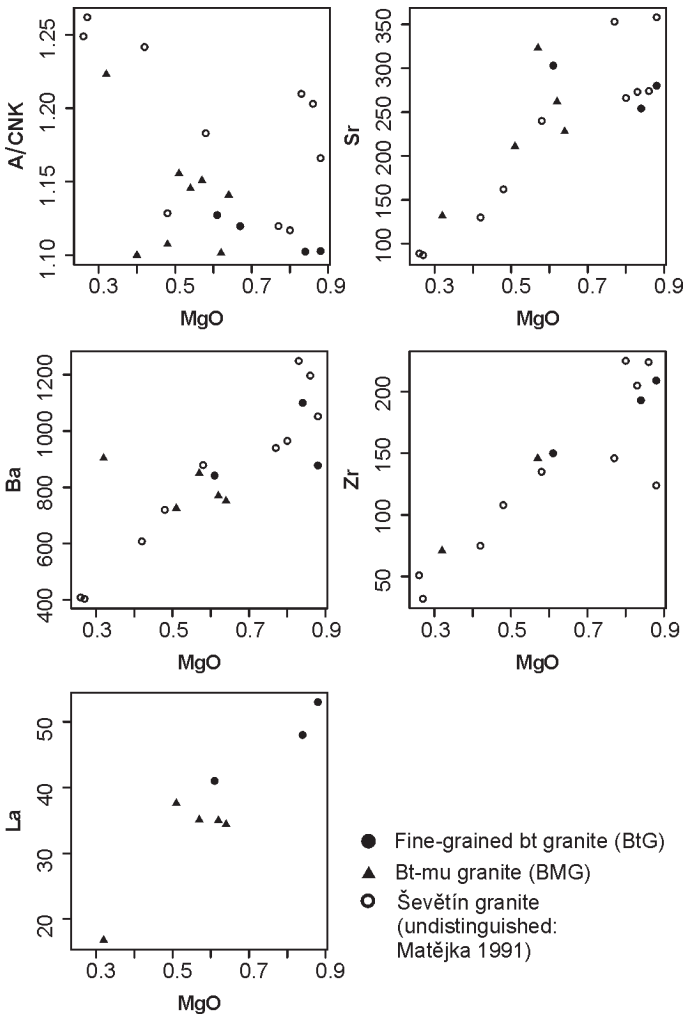

Fig. 11 Binary diagrams MgO versus selected trace elements (ppm) and the Shand's index (A/CNK) for Ševětín granites.

those for typical peraluminous granites of the Eisgarn family (represented for instance by the Deštná granites from the southern Ševětín Massif, whose mean A/CNK is 1.31 – Table 2). We cannot agree, though, that the fairly low A/CNK ratio of the Ševětín granites is caused by the absence of andalusite (cf. René *et al.* 1999).

Age constraints

The earlier petrologic and geochemical classification schemes for the Moldanubian Batholith (Holub *et al.* 1995, Klečka – Matějka 1996, Koller – Klötzli 1998 and references therein) all assign the late granitoids of I or transitional I/S chemistry (among others the Freistadt and Mauthausen intrusions) to a single group that has been usually considered to be substantially older than the strongly peraluminous, typical S type Eisgarn granites. This concept is based on results of relatively early Rb–Sr whole-rock dating. Alas these ages are not reliable, as they are frequently much too high, contradicting the field evidence. Some of the reconnaissance Rb–Sr ages reached 350 Ma or more (Mauthausen: 349 ± 4 Ma and 353 ± 5 Ma – Scharbert 1987, Mauthausen: 365 ± 8 Ma, Freistadt: 378 ± 8 Ma – Scharbert 1988) and were correctly recognized as being spurious, corresponding to mixing lines resulting from open-system processes (Scharbert 1988, Gerdes 1997).

The more recent U–Pb monazite dating confirmed a young age for the Freistadt granodiorite (302 ± 2 Ma: Friedl *et al.* 1992) and similar within the error age yielded the Rb–Sr WR dating of the Pfahl granite (312 ± 9 Ma: Gerdes 1997) as well as monazite electron microprobe dating of the Mauthausen granite (305 ± 10 Ma: Finger *et al.* 1996).

Moreover, the map of the Moldanubian Batholith shows the granites and granodiorites of the Mauthausen Group (Frasl – Finger 1991) as conspicuous arrays of elongated bodies, following the pattern of some major extension faults in the Moldanubian Zone of Lower Austria and southern Bohemia (cf. Brandmayr *et al.* 1995). The geological coincidence in place and time of some of these intrusions shows that their emplacement took place into relatively cold and brittle crust, only after opening of some major extensional fault structures in late Carboniferous, during a major E–W oriented extension (Brandmayr *et al.* 1995).

With reference to the absolute dating and the geological indication of a rather late emplacement, we confirm the idea of Finger *et al.* (1997) that at least some members of the Mauthausen group are late Variscan, younger than the strongly peraluminous two-mica granites of the Eisgarn clan (group EsP of Gerdes 1997). However, still considerable quantity of zircon and/or monazite dating will be necessary, before ages of all the granite types included in the Mauthausen group are established.

Likewise, the relatively young age of the Ševětín granite is supported by:

(1) Occurrence next to a major regional fault (i.e., Drahotěšice Fault, belonging to the fault pattern of the NNE–SSW oriented Blanice Graben),

(2) Presence of minute acicular or long-prismatic zircon and apatite crystals, indicating a rapid cooling and solidification, i.e. a shallow emplacement level,

(3) All the analyses recast to Improved Granite Mesonorm of Mielke – Winkler (1979) plot very close to low pressure (1–2 kbar), (nearly) water-saturated minimum in the normative Ab–Qz–Or triangle (after Johannes – Holtz 1996) compatible with crystallization close to the surface (Fig. 13),

(4) Unlike in the BMG, no effects of cataclastic and notable dynamic deformation have been observed in the biotite granite (BtG). This may possibly suggest that BtG was emplaced relatively late, following a gross part of deformations associated with movements along the Drahotěšice Fault Zone.

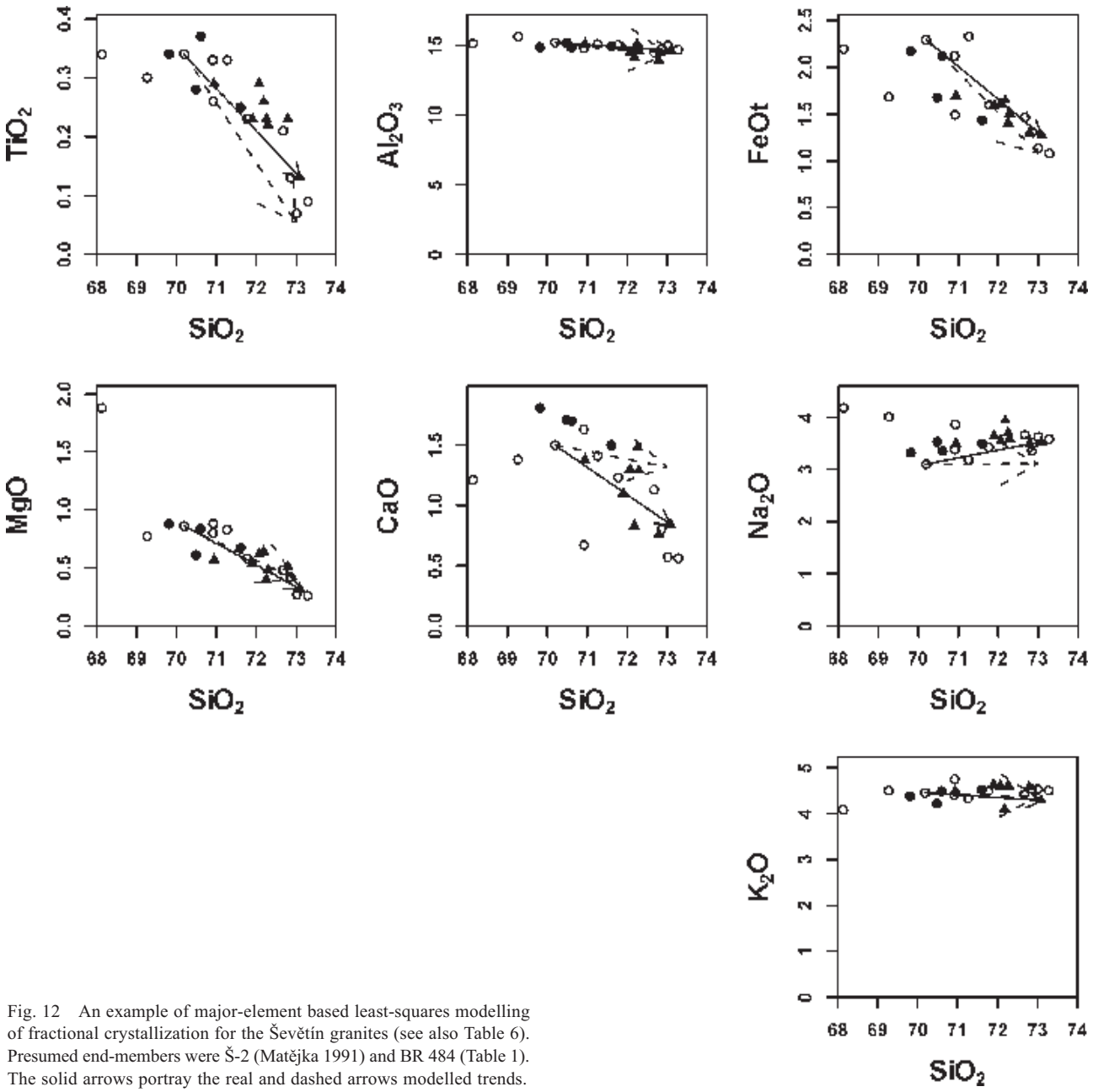

Fig. 12 An example of major-element based least-squares modelling of fractional crystallization for the Ševětín granites (see also Table 6). Presumed end-members were Š-2 (Matějka 1991) and BR 484 (Table 1). The solid arrows portray the real and dashed arrows modelled trends.

Source of the Ševětín granites

Concerning the petrogenesis of the Mauthausen Group granitoids, the early model of Liew *et al.* (1989) ascribed a key role to progressive lower crustal contamination of originally fairly primitive melts. For the relatively Sr-rich and Nd-poor Freistadt granodiorites it would have a profound effect on the Nd isotopic ratios, with the Sr isotopic ratios remaining largely unaffected. This scenario elucidates the highly negative ε^{i}_{Nd} values coupled with relatively unevolved $^{87}Sr/^{86}Sr_{i}$ ratios known from the Freistadt granodiorites. Moreover, the putative lower crustal contaminant would itself tend to have rather unradiogenic Sr isotopic signature due to its likely long-term impoverishment in Rb. Liew *et al.* (1989) assumed some depleted mantle input, at least indirectly, as a heat source.

In contrast, Vellmer – Wedepohl (1994) proposed for the Mauthausen granite a single, lower crustal metatonalitic source. According to these authors, this would have been essentially the same as that presumed for the Weinsberg granite; only the degree of melting would have to be higher (30–40 %).

Also Gerdes (1997) sought the main source of the Mauthausen Group granitoids in heterogeneous but at the same time quite primitive (tonalitic) crustal sources. He attributed an important role to enriched-mantle melts that could have been two-fold, as a source of quartz dioritic rocks associated with the Mauthausen Group, and as a heat source causing, due to late Variscan thinning and/or lithospheric mantle delamination, a widespread anatexis.

Finger *et al.* (1997) have ruled out a generally applicable direct subduction-related origin for the calc-alka-

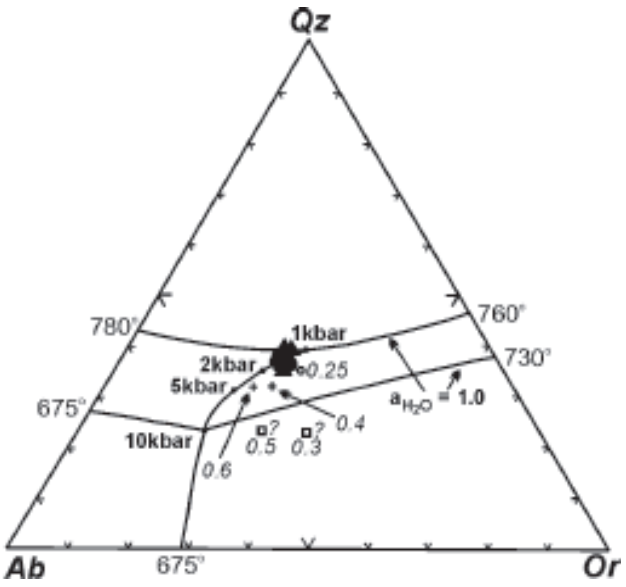

Fig. 13 The mesonormative (Mielke – Winkler 1977) Ab–Qz–Or ternary plot (Johannes – Holtz 1996, Fig. 2.20) showing the compositions of eutectics and minima in this system at various pressures (1, 2, 5 and 10 kbar) as well as water activities. H_2O saturated melts: full circles labelled by pressures; H_2O undersaturated melts at 2 kbar – empty circles, at 5 kbar – crosses and 10 kbar – empty squares. Plotted are analyses for samples of Ševětín granites collected during the present study.

line granitoids of the Mauthausen Group and similar intrusions within the Central European Variscides (cf. Finger – Steyrer 1990), arguing that there is no evidence for an ocean along the northern flank of the Variscan belt in Bohemian Massif *c.* 300 Ma ago. Finger *et al.* (1997) ascribed a crucial role to basic melts, possibly generated by remelting of relic oceanic crust following deeper burial and/or detachment of a fossil subduction zone. These melts were assumed to have become greatly contaminated during their ascent through the thickened crust. As an alternative, Finger *et al.* (1997 and references therein) discussed melting of enriched lithospheric mantle due to post-orogenic uplift and adiabatic decompression but they assumed that such a scenario is probably more applicable to the Aar Massif than to Eastern Alps and Western Carpathians where most of the late high–K calc-alkaline intrusions are encountered.

The petrologic and whole-rock geochemical character (weakly peraluminous, rather low K_2O/Na_2O, high Sr and Ba, low Rb, strongly negative ε^i_{Nd} at relatively unevolved $^{87}Sr/^{86}Sr_i$) of the Ševětín granites argues, at the first glimpse, for a quartzo–feldspathic source (arkose, graywacke, or granitic orthogneiss – Barbarin 1996 and references therein) fairly immature in terms of its major- and trace-element composition, and with relatively low time-integrated Sm/Nd and Rb/Sr ratios. The presence of cordierite, even though today largely pinitized, probably indicates a high–T, quite dry conditions of melting (Barbarin 1996).

The distinction between melts produced from metapsammitic parents and derived by anatexis of K-rich orthogneisses (metamorphosed syenogranite or monzogranite) is fairly difficult (e.g., Barbarin 1996, Sylvester 1998) even though the presence of metasedimentary enclaves and absence of mafic microgranular enclaves seem to be more compatible with the former. In any case, a more basic, K-poor metaigneous source (e.g., metatonalite assumed by Vellmer – Wedepohl 1994 and Gerdes 1997) can be discounted as its dehydratation melting would produce trondhjemic (at lower degrees of partial melting) to tonalitic and not granitic liquids (Johannes – Holtz 1996 and references therein).

The metapsammitic parentage for the Ševětín granites may be corroborated by their high CaO/Na_2O ratios (mean for BMG is 0.31, for BtG 0.49). As shown by Sylvester (1998), the pelite-derived post-collisional peraluminous granites have, due to their low initial contents of plagioclase and retention of Ca in the residual garnet in course of melting, CaO/Na_2O generally < 0.3. This is not fulfilled for the Ševětín granites but is indeed the case for Deštná (mean CaO/Na_2O = 0.12). Moreover, the Ševětín granites are also characterized by fairly low mean Al_2O_3/TiO_2 ratios (BtG: 48.6, BMG: 65.9) as compared to the Deštná granite (average Al_2O_3/TiO_2 = 226.2). These two parameters indicate that the BtG (± BMG) may have crystallized from a relatively hot metapsammite-derived melt, but the Deštná granite has a character of a typical pelite-derived granitic magma (see Figs 3 and 4 in Sylvester 1998). Such a conclusion would be also in line with the fact that Rb/Sr ratio in the Ševětín granites is close to, or somewhat less than, the unity (BtG: 0.74, BMG: 1.12). Again, this is in a sharp contrast to the Deštná granite, whose mean Rb/Sr = 2.8. Similarly, the mean Rb/Ba ratio of the Ševětín granites is fairly low (BtG = 0.22, BMG = 0.25) relative to the Deštná granite (Rb/Ba = 0.74) (see Fig. 7 of Sylvester 1998).

Hence it is clear that the source for Ševětín granites had to be distinct from that of the strongly peraluminous, often andalusite- and/or cordierite-bearing granites of the Eisgarn clan with significantly higher (less negative) ε^i_{Nd} and $^{87}Sr/^{86}Sr_i$. The difficulty is that such a metapsammitic source for the Ševětín granites is so far purely hypothetical, as its isotopic composition would have to have been different – inasmuch the available Sr–Nd isotope analyses permit us to judge – from the common Moldanubian metasediments (Fig. 8).

Another possibility is that the Rb depletion of the source was secondary, due to a loss of LILE into a melt or fluid phase. This scenario would invoke a high-grade, possibly granulitic protolith that would have to be essentially different from the (mainly acidic) granulites occurring in the Gföhl unit that are not LILE depleted (Pin – Vielzeuf 1983, Fiala *et al.* 1988) and show very different Sr–Nd isotopic signature (Fig. 8 and Vrána – Janoušek 1999). The depletion event would need to have taken place *long afore* the wake of Variscan orogeny to allow enough time for *in situ* growth of the observed low $^{143}Nd/^{144}Nd$ and $^{87}Sr/^{86}Sr$ ratios. Again, such a parental composition is – with our current knowledge of the

Moldanubian unit of the Bohemian Massif – purely hypothetical.

Lastly, the Sr–Nd isotopic composition of the Ševětín granites may reflect a mixing between two reservoirs: (1) a relatively primitive component, characterized by low time-integrated Rb/Sr and Sm/Nd ratios (i.e. LILE-depleted lower crustal rocks like in the previous case, relatively old, lower-grade metabasic rocks or even mantle-derived melts whose low Rb/Sr ratios would be a primary feature) and (2) a material geochemically and isotopically corresponding to mature Moldanubian metasedimentary rocks or their melts (Fig. 8). Similar scenario has been invoked already by Matějka – Janoušek (1998), who have ascribed the conspicuous linear alignment of analyses from several late granite intrusions of the MB (Pavlov, Bílý kámen, Boršov, Čeřínek) in the $^{87}Sr/^{86}Sr_i$ vs. ε^i_{Nd} and 1/Sr vs. $^{87}Sr/^{86}Sr_i$ diagrams to open-system processes. They assumed interaction of Sr from two sources, one unevolved ($^{87}Sr/^{86}Sr_i \leq 0.705$, $\varepsilon^i_{Nd} > -7$, Sr > 400 ppm), isotopically similar to, or more primitive than, Pavlov granite, and one evolved, close in composition to typical granites of the Eisgarn family or local metasediments (Moldanubian paragneisses). The analyses of the Ševětín granites fall more or less onto a straight line defined by the $^{87}Sr/^{86}Sr_i$ – ε^i_{Nd} isotopic data for above granite types (Fig. 8), most of them close to Boršov data points, and thus it is very tempting indeed to assume a similar genesis.

The viable scenarios explaining the mechanism of the binary mixing comprise:

(1) Pre-existing large-scale heterogeneity of the crustal sources to individual intrusions/magma batches. Prior to the onset of melting, both components could have been mixed already or could have been interlayered in various proportions – e.g. clastic sediments from several distinct sources, hybrid metaigneous rocks, or metasediments with intercalations of metabasic rocks,

(2) Relatively deep magma mixing. This would have to have been followed in some cases (such as Boršov or most of the Ševětín granites) by re-homogenization of each magmatic pulse *en route* to the higher crustal levels (in a hypothetical intermediate magma chamber) to account for their uniform Sr–Nd isotopic signature, or,

(3) An early assimilation of metasediments by quite primitive, possibly mantle-derived melts (more pronounced in more fractionated, i.e. relatively Sr-poor magmas).

As argued above, the presence of cordierite points to a high–T dehydratation melting of quartzo-feldspathic sources with or without a metabasic admixture. This is in line with the presumed low fertility of the Moldanubian crust following the generation of large volumes of two-mica granites of the Eisgarn group and would require the participation of mantle melts acting as a heat source (Barbarin 1996, Finger *et al.* 1997).

Were the mantle-derived magma also involved directly, the binary mixing between mantle and crustal components could be modelled reversibly to place some constraints on the nature of possible end-member compositions. In Fig. 14 a theoretical mixing hyperbola is plotted (least-squares method – Albarède 1995, see Appendix 1 for the R language programme) fitted through the data points for the Plöcking and Freistadt intrusions in Austria (Gerdes 1997 and references therein), as well as Pavlov (Matějka – Janoušek 1998) and Ševětín granites (this study) in the Czech Republic. Shown are also compositions of the Depleted Mantle (McCulloch – Blake 1984, Michard *et al.* 1985) and a typical Moldanubian paragneiss (Janoušek *et al.* 1995).

As the least-squares solution of the inverse mixing problem, we have obtained a hyperbola with asymptotes x = 0.70473 and y = –9.09, and curvature factor K = 0.004313 (see Albarède 1995 for terminology and required mathematic apparatus). This would imply an important conclusion that the more primitive end-member could not have been derived from Depleted Mantle or by remelting of little altered, relatively young MORB-like basalts. Instead CHUR-like or even slightly enriched mantle is to be envisaged. On the other hand, the mantle component would have to be much more primitive than enriched lithospheric mantle whose role was crucial in the genesis of earlier, highly potassic suites within the Moldanubian unit (Rastenberg intrusion: Gerdes *et al.* 2000, durbachite suite: Janoušek *et al.* 1995, 1997, Holub 1997).

Such a scenario would be capable of explaining the whole compositional spectrum observed for the Plöcking, Freistadt, Boršov and Ševětín intrusions. However, the

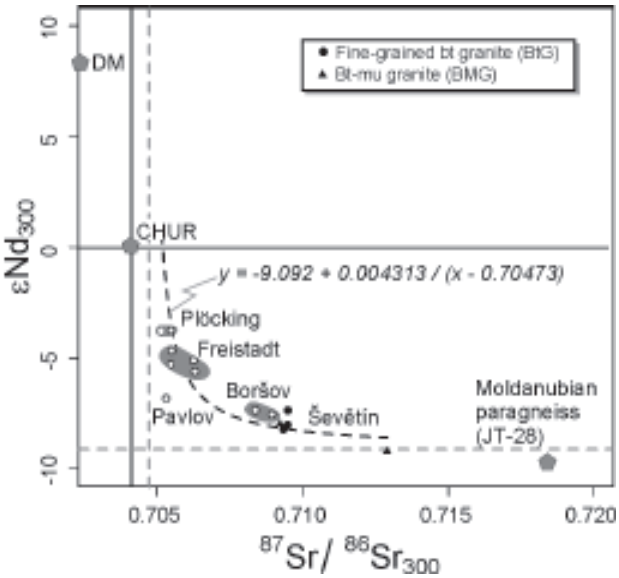

Fig. 14 Theoretical mixing hyperbola fitting data points for granitoids of the Plöcking and Freistadt intrusions (Gerdes 1997 and references therein), Pavlov granite (Matějka – Janoušek 1998) and Ševětín granite (this study). See the text for discussion and Appendix 1 for the least-squares modelling routine. Two asymptotes for the model hyperbola are shown by dashed lines. Depleted Mantle (DM) composition is from McCulloch – Blake (1984 – Sr) and Michard *et al.* (1985 – Nd); plotted is also an analysis of a typical Moldanubian paragneiss JT-28 (Janoušek *et al.* 1995).

compositions of the Pfahl and Mauthausen masses do not fit the mixing hyperbola at all, being shifted to more radiogenic Sr compositions (see also Fig. 8). This may point towards a somewhat different genesis (at least a different crustal end member with less negative ε^{i}_{Nd}. Also the composition of the Pavlov granite seems to show that the process could have been more complicated than assumed on the basis of the simplistic mathematical model.

Regardless of its exact mechanism, the binary mixing between two geochemically and isotopically distinct end-members is the most elegant hypothesis in that it assumes a single and realistic petrogenetic process to be responsible for generation of the full observed compositional range of the late Czech Moldanubian granites. Moreover, it accounts for higher $^{87}Sr/^{86}Sr_i$ and lower ε^{i}_{Nd} for the Ševětín sample BR 474 that would be otherwise difficult to explain.

Later history and genetic link between both granite types

Matějka (1991) explained the origin of the fine-grained biotite granite (BtG) in Ševětín by two alternative scenarios. The first proposed the BtG to be a more contaminated version of the coarser-grained biotite–muscovite granite (BMG). This hypothesis can be discounted with confidence in the light of our new Sr-Nd isotopic data. Given that it is extremely unlikely that contaminant had an identical isotopic composition as the parental magma and that its proportions in all sampled rocks were exactly the same, the mostly remarkably uniform Sr-Nd isotopic ratios showing no pronounced differences between both rock types argue strongly against operation of such a process.

This said it is worth noting that there are slight but significant and systematic variations in initial Nd isotopic compositions, if plotted against some suitable fractionation index (such as SiO_2 – Fig. 15). The less siliceous samples show lower $^{143}Nd/^{144}Nd_{300}$ ratios (corresponding to more negative ε^{300}_{Nd} values) than the more siliceous ones. The $SiO_2 - ^{87}Sr/^{86}Sr_{300}$ plot (Fig. 16) does not show such a clear systematic trend but the scatter of data points is still higher than it could be accounted for by analytical errors only.

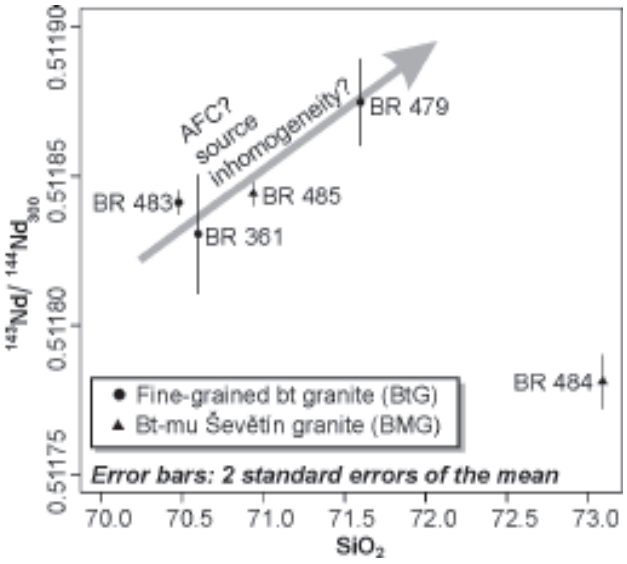

Fig. 15 SiO_2 versus $^{143}Nd/^{144}Nd_{300}$ graph for the Ševětín granites. Hypothetical effects of assimilation or source inhomogeneity are also plotted.

One possible explanation would be that the observed Nd isotopic data array portrays heterogeneities inherited from the source and that individual magma batches failed to rehomogenize thoroughly. If the studied granites are virtually devoid of restite, the observed correlation with silica would imply that the whole compositional spectrum of the Ševětín granites resulted solely from various degrees of partial melting which is at variance with the observed sharp drop in biotite and feldspar-compatible LILE (Ba and Sr) and some HFSE controlled by saturation of accessory phases (Zr, Th, LREE) with increasing silica. These trends in fact bear – as confirmed by numerical modelling – an evidence for important petrogenetic role of fractional crystallization (see preceding section).

With the notable exception of the sample BR 474, the Sr–Nd isotopic variation within the intrusion hence implies some, but only a finite, role for open-system processes, such as magma mixing or (high-level) country-rock assimilation. Similar conclusion concerning the genesis of granitoids of the Mauthausen Group was drawn also by Gerdes (1997) on the basis of his own as well as previously published (Scharbert 1988) Sr–Nd isotopic data. Regarding the late assimilation, this process is usually accompanied by fractional crystallization (AFC: De Paolo 1981). For Ševětín, the rather inconspicuous Sr–Nd isotopic effects signify – in agreement with presumed fairly low thermal energy of relatively cool magma intruding the shallow crustal levels – that the fractional crystallization could have been attended with only severely restricted degree of assimilation (low value of *r*, i.e. rate of assimilation to fractional crystallization – De Paolo 1981). This crystallization-dominated process would then inevitably drive the magma composition towards higher silica contents. If true, Figs 14 and 15 imply that the contaminant would need to have been relatively primitive ($^{87}Sr/^{86}Sr_{300}$ of 0.709 or less, and ε^{300}_{Nd} higher, i.e. less negative, than *c.* –7) compared to the parental magma and known isotopic compositions of the surrounding Moldanubian metasedimentary rocks (Fig. 8). On this basis, the assimilation model is either invalid or the contaminant corresponded to a so far unsampled or on the present intrusion level unknown lithology.

As a second genetic scenario Matějka (1991) proposed that the BtG corresponds to an earlier, less evolved magma pulse from a common magma chamber. This earlier facies (or even 'chilled margin' as Matějka 1991 speculated) would have been later disrupted by the more fractionated pulse (BMG). This is a viable hypothesis indeed, as there are not really significant Sr–Nd isotopic differences between both types (with exception of BR 484, of course), whole-rock geochemical compositions and pet-

rographic character of BtG and BMG do overlap and, as shown by numerical modelling, both rock types can be linked mainly by a simple fractional crystallization process. The observed minor Nd isotopic heterogeneity could then be explained by an influx and intermixing of slightly isotopically and geochemically different melts into periodically replenished, periodically tapped, continuously fractionated magma chamber (RTF: O'Hara 1977, O'Hara – Matthews 1981).

Conclusions

(1) The whole-rock geochemical signature of the BtG is less evolved than that of the BMG. The former shows lower SiO_2, Na_2O, K_2O and A/CNK accompanied by higher TiO_2, FeO_t, MgO, Al_2O_3 and CaO. The BtG is also characterized by higher contents of Rb, Sr, Cr, Ni, La, LREE, Eu and Zr than the BMG.

(2) Overall, the mode of occurrence, as well as major- and trace-element whole-rock geochemical signature of the Ševětín granites strongly resemble that of the Mauthausen granite in Austria.

(3) The initial Sr isotopic ratios for most of the samples are nearly uniform, showing fairly evolved character of the parental magmas ($^{87}Sr/^{86}Sr_{300}$ = 0.70922–0.70950). Notable exception is the sample BR 484 (BMG, $^{87}Sr/^{86}Sr_{300}$ = 0.71290).

(4) The initial epsilon Nd values are all highly negative (ε_{Nd}^{300} = –7.4 to –8.0; BR 484: ε_{Nd}^{300} = –9.2). This is reflected by high Depleted Mantle model ages (two-stage T_{DM}^{Nd} = 1.60–1.75 Ga).

(5) Both Ševětín granites (BtG and BMG) are coeval. Their Sr–Nd isotopic compositions and geochemical character correspond to a quartz–feldspathic (?metapsammitic) parentage or, more likely, may reflect a mixing between a relatively primitive component (characterized by a long-term depletion in LILE and having low time-integrated Rb/Sr and Sm/Nd ratios, with $^{87}Sr/^{86}Sr_i \leq 0.705$ and $\varepsilon_{Nd}^{i} > -7$, such as (undepleted or slightly enriched) mantle-derived melts or metabasic rocks) and a material geochemically corresponding to mature Moldanubian metasedimentary rocks or their melts ($^{87}Sr/^{86}Sr_i > 0.713$ and $\varepsilon_{Nd}^{i} < -9.5$).

(6) Both BtG and BMG can be linked by (nearly) closed system fractional crystallization of biotite slightly prevailing over plagioclase.

(7) The observed minor Nd isotopic heterogeneity (with $^{143}Nd/^{144}Nd$ ratios correlating positively with silica contents) could be explained most satisfactorily by an influx of slightly isotopically and geochemically different melt batch(es) into periodically tapped and replenished magma chamber.

(8) The Ševětín granites are probably fairly late, with indirect evidence indicating their age similar to Mauthausen Group in Austria (~ 300 Ma). This statement is consistent not only with comparable whole-rock geochemistry and Sr isotopic compositions of the Ševětín and Mauthausen granites (even though the Nd isotopic signatures of the two do differ profoundly) but also with occurrence of Ševětín granites close to late major regional fault forming a part of Blanice Graben generated during the late Variscan extensional collapse. Moreover, the shallow intrusion level is supported also by the morphology of minute zircon and apatite crystals indicating a rapid cooling and solidification, and the Ab–Qz–Or normative compositions.

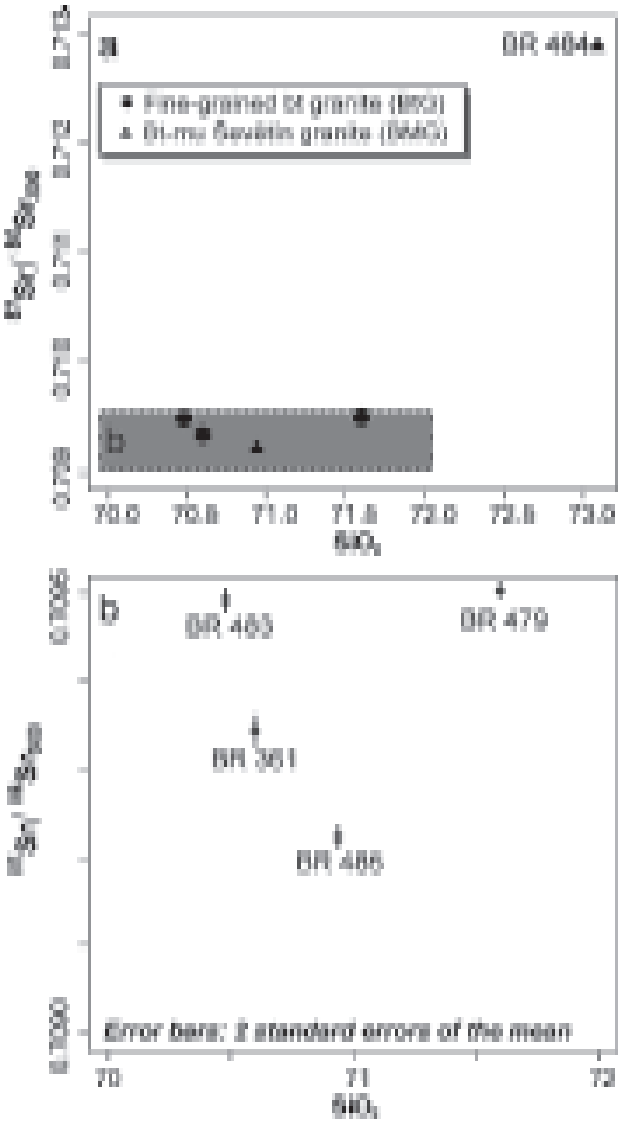

Fig. 16 SiO_2 versus $(^{87}Sr/^{86}Sr)_{300}$ graph for the Ševětín granites. In the blown up portion of the diagram (inset) are shown error bars corresponding to ± 1 standard error of the mean.

Acknowledgements. We are indebted to D. Matějka (Prague) for permission to use his extensive database of unpublished data for granitoids from the Czech part of the Moldanubian Batholith, Getrude Friedl (Salzburg) and František V. Holub (Prague) for a careful and thoughtful reviews, Fritz Finger (Salzburg) for enlightening discussions and J. Trnková, with V. Kopecký and J. Zeman for technical assistance.

Submitted December 19, 2001

References

Albarède, F. (1995): Introduction to geochemical modeling. – University Press, Cambridge, 543 pp.

Ambrož, V. (1935): Studie o krystaliniku mezi Hlubokou a Týnem nad Vltavou. – Spisy přírodověd. Fak. Univ. Karl., 138: 1–44.

Ayres, M. – Harris, N. (1997): REE fractionation and Nd-isotope disequilibrium during crustal anatexis: constraints from Himalayan leucogranites. – Chem. Geol., 139: 249–269.

Barbarin, B. (1996): Genesis of the two main types of peraluminous granitoids. – Geology, 24: 295–298.

Blundy, J. D. – Shimizu, N. (1991): Trace element evidence for plagioclase recycling in calc-alkaline magmas. – Earth Planet. Sci. Lett., 102: 178–197.

Boynton, W. V. (1984): Cosmochemistry of the rare earth elements: meteorite studies. – *In:* Henderson, P. (ed.): Rare Earth Element Geochemistry. Elsevier, Amsterdam, 63–114.

Brandmayr, M. – Dallmeyer, R. D. – Handler, R. – Wallbrecher, E. (1995): Conjugate shear zones in the southern Bohemian Massif (Austria): implications for Variscan and Alpine tectonothermal activity. – Tectonophysics, 248: 97–116.

Breiter, K. – Scharbert, S. (1995): The Homolka Magmatic Centre – an example of Late Variscan ore bearing magmatism in Southbohemian Batholith (Southern Bohemia, Northern Austria). – Jb. Geol. B.-A., 138: 9–25.

Broska, I. – Uher, P. (2001): Whole-rock chemistry and genetic typology of the West- Carpathian Variscan granites. – Geol. Carpath., 52: 79–90.

Bryan, W. B. – Finger, L. W. – Chayes, F. (1969): Estimating proportions in petrographic mixing equations by least-squares approximation. – Science, 163: 926–927.

Buccianti, A. – Peccerillo, A. (1999): The complex nature of potassic and ultrapotassic magmatism in Central-Southern Italy: a multivariate analysis of major element data. – *In:* Lippard, S. J. *et al.* (eds): Proceedings of the 5th Annual Conference of the International Association for Mathematical Geology. Tapir, Trondheim, 145–150.

Chappell, B. W. – White, A. J. R. – Wyborn, D. (1987): The importance of residual source material (restite) in granite petrogenesis. – J. Petrology, 28: 571–604.

Cordier, P. – Vrána, S. – Doukhan, J. C. (1994): Shock metamorphism in quartz at Sevetin and Susice (Bohemia)? A TEM investigation. – Meteoritics, 29: 98–99.

D'Amico, C. – Rottura, A. – Bargossi, G. M. – Nannetti, M. C. (1981): Magmatic genesis of andalusite in peraluminous granites. Examples from Eisgarn type granites in Moldanubicum. – Rc. Soc. ital. Mineral. Petrologia, 38: 15–25.

De Paolo, D. J. (1981): Trace element and isotopic effects of combined wallrock assimilation and fractional crystallization. – Earth Planet. Sci. Lett., 53: 189–202.

De La Roche, H. – Leterrier, J. – Grandclaude, P. – Marchal, M. (1980): A classification of volcanic and plutonic rocks using R_1R_2 – diagram and major element analyses – its relationships with current nomenclature. – Chem. Geol., 29: 183–210.

Fiala, J. – Matějovská, O. – Vaňková, V. (1988): Bohemian Massif granulites – possible representatives of anomalous lower crust. – Phys. Earth Planet. Inter., 51: 125–127.

Fiala, J. – Fuchs, G. – Wendt, J. I. (1995): VII.C.1. Moldanubian Zone – Stratigraphy. – *In:* Dallmeyer R. D. *et al.* (eds): Pre-Permian Geology of Central and Eastern Europe. Springer, Berlin, 417–428.

Finger, F. – Steyrer, H. P. (1990): I-type granitoids as indicators of a late Paleozoic convergent ocean–continent margin along the southern flank of the central European Variscan orogen. – Geology, 18: 1207–1210.

Finger, F. – Benisek, A. – Broska, I. – Haunschmid, B. – Schermaier, A. – Schindlmayr, A. – Schitter, F. (1996): Alterdaten von Monaziten mit der Elektronenmikrosonde. – 6. Symposion Tektonik–Strukturgeologie–Kristallingeologie, Salzburg, 100–102.

Finger, F. – Roberts, M. P. – Haunschmid, B. – Schermaier, A. – Steyrer, H. P. (1997): Variscan granitoids of central Europe: their typology, potential sources and tectonothermal relations. – Min. Petrol., 61: 67–96.

Frasl, G. – Finger, F. (1991): Geologisch-petrographische Exkursion in den österreischischen Teil des Südböhmischen Batholiths. – Eu. J. Mineral. 3/2, 23–40.

Friedl, G. – von Quadt, A. – Frasl, G. – Finger, F. (1992): Neue U/Pb Altersdaten aus der südlichen Böhmischen Masse. – Frankfurter Geowiss. Arb.: A11, 217–218.

Friedl, G. – von Quadt, A. – Finger, F. (1996): Timing der Intrusionstätigkeit im Südböhmischen Batholith: 6. Symposion Tektonik-Struktur-geologie-Kristallingeologie, Salzburg, 127–130.

Gabriel, K. R. (1971): The biplot graphical display of matrices with application to principal component analysis. – Biometrika 58: 453–467.

Gerdes, A. (1997): Geochemische und thermische Modelle zur Frage der spätorogenen Granitgenese am Beispiel des Südböhmischen Batholiths: Basaltisches Underplating oder Krustenstapelung? – Unpublished Ph.D. thesis, Univ. Göttingen. pp 113.

Gerdes, A. – Wörner, G. – Finger, F. (2000): Hybrids, magma mixing and enriched mantle melts in post-collisional Variscan granitoids: the Rastenberg Pluton, Austria. – *In:* Franke, W. *et al.* (eds): Orogenic Processes: Quantification and Modelling in the Variscan Fold Belt. Geological Society, London, Special Publication 179, London, 415–431.

Harvey, P. K. – Atkin, B. P. (1981): The rapid determination of Rb, Sr and their ratios in geological materials by X-ray fluorescence spectrometry using a rhodium X-ray tube. – Chem. Geol., 32: 155–165.

Holub, F. V. (1997): Ultrapotassic plutonic rocks of the durbachite series in the Bohemian Massif: Petrology, geochemistry and petrogenetic interpretation. – Sbor. geol. Věd, ložisk. Geol. Mineral., 31: 5–26.

Holub, F. V. – Klečka M. – Matějka D. (1995): VII.C.3. Moldanubian Zone – Igneous Activity. – *In:* Dallmeyer R. D. *et al.* (eds): Pre-Permian Geology of Central and Eastern Europe. Springer, Berlin, 444–452.

Icenhower, J. – London, D. (1995): An experimental study of element partitioning among biotite, muscovite and coexisting peraluminous silicic melt at 200 MPa (H_2O). – Amer. Mineralogist, 80: 1229–1251.

Ihaka, R. – Gentleman, R. (1996): R: A language for data analysis and graphics. – J. Comput. Graph. Statistics 5: 299–344.

Jacobsen, S. B. – Wasserburg, G. J. (1980): Sm–Nd evolution of chondrites. – Earth Planet. Sci. Lett., 50: 139–155.

Janoušek, V. (2000a): Interpretation of the whole-rock geochemical data using the R language – the current state of affairs. – *In:* Uher, P. *et al.* (eds). Mineralogicko-petrologické sympózium Magurka '2000, 16.

– (2000b): R – an alternative to spreadsheets and special software for geochemical calculations and plotting. – Geolines, 10: 34–35.

Janoušek, V. – Rogers, G. – Bowes, D. R. (1995): Sr–Nd isotopic constraints on the petrogenesis of the Central Bohemian Pluton, Czech Republic. – Geol. Rundsch., 84: 520–534.

Janoušek, V. – Holub, F. V. – Rogers, G. – Bowes, D. R. (1997): Two distinct mantle sources of Hercynian magmas intruding the Moldanubian unit, Bohemian Massif, Czech Republic. – J. Czech Geol. Soc., 42: 10.

Janoušek, V. – Bowes, D. R. – Rogers, G. – Farrow, C. M. – Jelínek, E. (2000): Modelling diverse processes in the petrogenesis of a composite batholith: the Central Bohemian Pluton, Central European Hercynides. – J. Petrology, 41: 511–543.

Johannes, W. – Holtz, G. (1996): Petrogenesis and experimental petrology of granitic rocks. – Springer, Berlin, 335 pp.

Klečka, M. – Matějka, D. (1996): Moldanubian Batholith – an example of the evolution of the Late Palaeozoic granitoid magmatism in the Moldanubian Zone, Bohemian Massif (Central Europe). – *In:* Srivastava, R. K. – Chandra, R. (eds): Magmatism in relation to diverse tectonic settings. Oxford & IBH Publishing Co., New Delhi, 353–373.

Klečka, M. – Matějka, D. – Jalovec, J. – Vaňková, V. (1991): Geochemický výzkum granitoidů typu Eisgarn v jižní části centrálního masívu moldanubického plutonu. – Zpr. geol. výzk. v roce 1989, 109–111.

Koller, F. – Klötzli, U. (1998): The evolution of the South Bohemian Pluton. – *In:* Breiter K. (ed.): Genetic significance of phosphorus in fractionated granites. Excursion guide. Czech Geological Survey, Prague, 11–14.

Košler, J. – Kelley, S. P. – Vrána, S. (2001): Ar/Ar hornblende dating of a microgranodiorite dyke: Implications for early Permian extension in the Moldanubian Zone of the Bohemian Massif. – Int. J. Earth Sciences (Geol. Rdsch.), 90: 379–385.

Kröner, A. – Hegner, E. – Hammer, J. – Haase, G. – Bielicki, K. H. – Krauss, M. – Eidam, J. (1994): Geochronology and Nd–Sr systematics of Lusatian granitoids – significance for the evolution of the Variscan orogen in East–Central–Europe. – Geol. Rundsch., 83: 357–376.

Liew, T. C. – Hofmann, A. W. (1988): Precambrian crustal components, plutonic associations, plate environment of the Hercynian Fold Belt of central Europe: indications from a Nd and Sr isotopic study. – Contrib. Mineral. Petrol., 98: 129–138.

Liew, T. C. – Finger, F. – Höck, V. (1989): The Moldanubian granitoid plutons in Austria: chemical and isotopic studies bearing on their environmental setting. – Chem. Geol., 76: 41–55.

Lugmair, G. W. – Marti, K. (1978): Lunar initial $^{143}Nd/^{144}Nd$: differential evolution line of the lunar crust and mantle. – Earth Planet. Sci. Lett., 39: 349–357.

Matějka, D. (1991): Geochemická a petrologická charakteristika hornin moldanubika jižně od Veselí nad Lužnicí a vztah šěvětínského granodioritu k horninám typu Eisgarn. – Unpublished PhD. thesis. Charles University, Prague. 148 pp. (in Czech).

Matějka, D. – Janoušek, V. (1998): Whole-rock geochemistry and petrogenesis of granites from the northern part of the Moldanubian Batholith (Czech Republic). – Acta Univ. Carol., Geol., 42: 73–79.

McCulloch, M. T. – Black, L. P. (1984): Sm-Nd isotopic systematics of Enderby Land granulites and evidence for the redistribution of Sm and Nd during metamorphism. – Earth Planet. Sci. Lett., 71: 46–58.

Michard, A. – Gurriet, P. – Soudant, M. – Albarède, F. (1985): Nd isotopes in French Phanerozoic shales: external vs. internal aspects of crustal evolution. – Geochim. Cosmochim. Acta, 49: 601–610.

Mielke, P. – Winkler, H. G. F. (1979): Eine bessere Berechnung der Mesonorm für granitische Gesteine. – Neu. Jb. Mineral., Mh., 471–480.

O'Hara, M. J. (1977): Geochemical evolution during fractional crystallisation of a periodically refilled magma chamber. – Nature, 266: 503–507.

O'Hara, M. J. – Matthews, R. E (1981): Geochemical evolution in an advancing, periodically replenished, periodically tapped, continuously fractionated magma chamber. – J. Geol. Soc., London, 138: 237–277.

Petrík, I. – Kohút, M. (1997): The evolution of granitoid magmatism in the Hercynian orogen in the Western Carpathians. – *In:* Grecula, P. *et al.* (eds): Geological Evolution of the Western Carpathians. Mineralia Slovaca – Monograph, Bratislava, 235–252.

Pin, C. – Vielzeuf, D. (1983): Granulites and related rocks in Variscan Median Europe: a dualistic interpretation. – Tectonophysics, 93: 47–74.

R Development Core Team (2001): The R Reference Index. Accessed November 29, 2001, at URL http://cran.r-project.org/doc/manuals/refman.pdf.

René, M. – Matějka, D. – Klečka, M. (1999): Petrogenesis of granites of the Klenov Massif. – Acta Montana, 113: 107– 134.

Richard, P. – Shimizu, N. – Allégre, C. J. (1976): $^{143}Nd/^{146}Nd$, a natural tracer: an application to oceanic basalts. – Earth Planet. Sci. Lett., 31: 269–278.

Scharbert, S. (1987): Rb–Sr Untersuchungen granitoider Gesteine des Moldanubikums in Österreich. – Mitt. Österr. mineral. Gesell., 132: 21–37.

– (1988): Rubidium–strontium systematics of granitoid rocks of the South Bohemian Pluton. – *In:* Kukal, Z. (ed.): Proceedings of the 1st International Conference on the Bohemian Massif. Czech Geological Survey, Prague, 229–232.

– (1998): Some geochronological data from the South Bohemian Pluton in Austria: a critical review. – Acta Univ. Carol., Geol., 42: 114–118.

Scharbert, S. – Veselá, M. (1990): Rb–Sr systematics of intrusive rocks from the Moldanubicum around Jihlava. – *In:* Minaříková, D. – Lobitzer, H. (eds): Thirty years of geological cooperation between Austria and Czechoslovakia. Czech Geological Survey, Prague, 262–271.

Scharbert, S. – Breiter, K. – Frank, W. (1997): The cooling history of the southern Bohemian Massif. – J. Czech Geol. Soc. 42: 24.

Steiger, R. H. – Jäger, E. (1977): Subcommission on geochronology: convention on the use of decay constants in geo- and cosmochronology. – Earth Planet. Sci. Lett. 36: 359–362.

Suk, M. et al. (1978): Explanations to the geological map of the Czech Republic 1 : 25 000, sheet 22–444, Ševětín. – Czech Geological Survey, Prague. 45 pp. (in Czech).

Sylvester, P. J. (1998): Post-collisional strongly peraluminous granites. – Lithos, 45: 29–44.

Uher, P. – Broska, I. (2000): The role of silicic magmatism in the Western Carpathians: from Variscan collision to Early-Alpine extension. – Slovak. Geol. Mag., 6: 278–280.

Valbracht, P. J. – Vrána, S. – Beetsma, J. J. – Fiala, J. – Matějka, D. (1994): Sr and Nd isotopic determinations in three Moldanubian granulite massifs in southern Bohemia. – J. Czech Geol. Soc., 39: 114.

Vellmer, C. – Wedepohl, K. (1994): Geochemical characterization and origin of granitoids from the South Bohemian Batholith in Lower Austria. – Contrib. Mineral. Petrol., 118: 13–32.

Vrána, S. – Janoušek, V. (1999): Geochemistry and petrogenesis of granulites in the Lišov Granulite Massif, Moldanubian Zone in Southern Bohemia. – Geolines, 8: 74.

Vrána, S. – Bendl, J. – Buzek, F. (1993): Pyroxene microgranodiorite dykes from the Ševětín structure, Czech Republic: mineralogical, chemical and isotopic indication of a possible impact melt origin. – J. Czech Geol. Soc., 38, 129–148.

Petrologie, geochemický charakter a petrogeneze pozdně variské granitové intruze: příklady ze ševětínského masívu, moldanubický pluton, jižní Čechy

V ševětínském masívu (moldanubická zóna, jižní Čechy) lze rozeznat tři intruzívní fáze: (1) nejstarší dvojslídné granity typu Deštná s cordieritem ± andalusitem (jv. část tělesa), (2) biotit–muskovitický ševětínský granit (BMG), tvořící většinu masívu a (3) jemnozrnný–drobnozrnný biotitický granit (BtG) budující jen malá tělesa.

Oba ševětínské granity vykazují znaky přechodného I/S typu. Geochemický charakter BtG je méně frakcionovaný než BMG. Biotitické granity mají nižší SiO_2, Na_2O, K_2O a A/CNK spolu s vyššími TiO_2, FeO_t, MgO, Al_2O_3 a CaO. Pro BtG jsou také charakteristické vyšší obsahy Rb, Sr, Cr, Ni, La, LREE, Eu a Zr než pro BMG.

Iniciální poměry Sr izotopů pro čtyři vzorky jsou navzájem velmi podobné bez ohledu na granitový typ (BtG/BMG) a ukazují na silně frakcionovanou krustální komponentu ($^{87}Sr/^{86}Sr_{300}$ = 0.70922–0.70950). Vzorek BR 484 má ještě radiogennější stroncium ($^{87}Sr/^{86}Sr_{300}$ = 0.71290). Iniciální hodnoty epsilon Nd jsou všechny silně negativní (ε_{Nd}^{300} = –7.4 až –8.0; BR 484: ε_{Nd}^{300} = –9.2), což odpovídá vysokým dvojstupňovým Nd modelovým stářím (T_{DM}^{Nd} = 1.60–1.75 miliard let).

Oba ševětínské granity jsou kogenetické, jejich Sr–Nd izotopický charakter ukazuje na derivaci z křemen-živcového zdroje (? metapsamit) nebo, pravděpodobněji, odráží míšení mezi dvěma komponentami: (1) relativně primitivní (s nízkými Rb/Sr a Sm/Nd poměry, $^{87}Sr/^{86}Sr_i \leq 0.705$ a $\varepsilon_{Nd}^{i} > -7$: např. taveniny derivované ze slabě obohaceného plášťového zdroje anebo metabazitů) a (2) materiálu geochemicky odpovídajícího zralým moldanubickým metasedimentům či jejich taveninám ($^{87}Sr/^{86}Sr_i > 0.713$ a $\varepsilon_{Nd}^{i} < -9.5$). Jak BtG tak i BMG jsou pravděpodobně geneticky spjaté *c.* 10 % frakční krystalizací biotitu a plagioklasu. Pozorovanou slabou, avšak systematickou, Nd izotopickou variaci lze vysvětlit přínosem izotopicky poněkud odlišnějších porcí magmatu do kontinuálně frakcionujícího magmatického krbu (RTF).

Ševětínské granity jsou pravděpodobně dosti pozdní; nepřímé důkazy ukazují značnou podobnost v petrologii, geochemickém charakteru a pravděpodobně i stáří s mauthausenskou skupinou moldanubického batolitu (~300 mil. let?). To odpovídá výskytu ševětínských granitů blízko významných pozdně variských extenzních zlomů blanické brázdy. Malá hloubka intruze a rychlé chladnutí jsou indikovány také přítomností velkého množství drobných, dlouze prizmatických krystalů zirkonu a apatitu, jakož i pozici ševětínských analýz v normativním diagramu Ab–Qz–Or.

Appendix 1 Least-squares solution for the inverse problem of binary mixing using the Sr–Nd isotopic compositions (R language implementation of the algorithm given by Albarède 1995)

The equation of a mixing hyperbola in the *[x, y]* space can be written in the form (Albarède 1995, p. 262):

$$(y - y_0)(x - x_0) = q \tag{1}$$

Where: x_0, y_0 = asymptotes, and q = curvature parameter

This can be rearranged to:

$$xy = q - x_0 y_0 + y x_0 + x y_0 \tag{2}$$

or a more familiar form:

$$y = y_0 + \frac{q}{x - x_0} \tag{3}$$

Let's build a matrix *A* with three columns, including 1, *x* and *y*. The vector *y* should contain products *xy*. Then balance can be written in a matrix form (Albarède 1995):

$$y = Ax \tag{4}$$

and solved for vector *x* containing the elements $[q\text{-}x_0y_0, x_0, y_0]$ by the least-squares method.

```
# The plain text, tab-delimited data file contains three columns:
# 1st = sample ID
# 2nd = initial Sr isotopic ratios
# 3rd = initial epsilon values

#read the data
   z<-as.matrix(read.table("mix.data",sep="\t"))

# calculate the results
   A<-cbind(1,z[,2],z[,1])
   y<-z[,1]*z[,2]
   xa<-lsfit(A,y,intercept=FALSE)
   xa<-xa$coefficients
   u<-xa[2]
   v<-xa[3]  # asympotes
   cc<-xa[1]+u*v   # curvature
# and print them
   X<-seq(min(z[,1]),max(z[,1]),by=0.00001)
   result<-paste("The best fit hyperbola is: y =",round(v,5),
   "+",round(cc,8),"/(x-",round(u,4),")",sep="")
   cat(result, "\n")

# plot the data and mixing hyperbola
   Y<-(cc-u*v+X*v)/(X-u)
   plot(X,Y,type="l",col="red",xlab="87Sr/86Sri",ylab="EpsNdi")
   points(z[,1],z[,2])

# plot asymptotes
   abline(h=v)
   abline(v=u)
```